(1995).
6) Rybak M. J., *Clin. Infect. Dis.*, **42**, S35—S39 (2006).
7) Le Normand Y., Milpied N., Kergueris M. F., Harousseau J. L., *Int. J. Biomed. Comput.*, **36**, 121—125 (1994).
8) Buelga D. S., Fernandez de Gatta M., Herrera E. V., Dominguez-Gil A., García M. J., *Antimicrob. Agents Chemother.*, **49**, 4934—4941 (2005).
9) Aldaz A., Ortega A., Idoate A., Giraldez J., Bougarolas A., *Ther. Drug Monit.*, **22**, 250—257 (2000).
10) Fernández de Gatta M., Fruns I., Hernández J. M., Caballero D., San Miguel J. F., Martínez Lanao J., Domínguez-Gil Hurlé A., *Clin. Pharm.*, **12**, 515—520 (1993).
11) Yasuhara M., Iga T., Zenda H., Okumura K., Oguma T., Yano Y., Hori R., *Ther. Drug. Monit.*, **20**, 139—148 (1998).
12) Jelliffe R. W., Schumitzky A., Bayard D., Milman M., Guilder M. V., Wang X., Jiang F., Barbaut X., Maire P., *Clin. Pharmacokinet.*, **34**, 57—77 (1998).
13) Teramachi H., Hatakeyama H., Matsushita R., Imai Y., Miyamoto K., Tsuji A., *Biol. Pharm. Bull.*, **25**, 1333—1338 (2002).
14) Ohnishi A., Yano Y., Shimamura K., Oguma T., *Biol. Pharm. Bull.*, **24**, 1446—1450 (2001).
15) Matzke G. R., "Applied Pharmacokinetics," 2nd ed., ed. by Evans W. E., Schentag J. J., Jusko W. J., Applied Therapeutics, Inc., Spokane, WA, 1986.
16) Chang D., Lime L., Malogolowkin M., *Pediatr. Infect. Dis. J.*, **13**, 969—974 (1994).
17) Krivoy N., Peleg S., Postovsky S., Arush M. W. B., *Pediatr. Hematol. Oncol.*, **15**, 333—338 (1998).
18) Chang D., *Pediatr. Infect. Dis. J.*, **14**, 667—673 (1995).
19) Teramachi H., Matsushita R., Tsuji A., *Jpn. J. Chemother.*, **53**, 357—363 (2005). (in Japanese except Abstract)
20) Cockcroft D. W., Gault M. H., *Nephron*, **16**, 31—41 (1976).
21) Sheiner L. B., Beal S. L., *J. Pharm. Sci.*, **71**, 1344—1348 (1982).
22) Yano Y., Oguma T., *Jpn. J. Ther. Drug Monit.*, **14**, 179—188 (1997). (in Japanese except Abstract).
23) Sheiner L. B., Beal S. L., *J. Pharmacokinet. Biopharm.*, **9**, 503—512 (1981).
24) Tsuchiwata S., Mihara K., Yafune A., Ogata H., *Ther. Drug Monit.*, **27**, 18—24 (2005).
25) Mahmood I., *Int. J. Clin. Pharmacol. Ther.*, **41**, 392—396 (2003).
26) Ohnishi A., Yano Y., Ishibashi T., Katsube T., Oguma T., *Drug Metab. Pharmacokinet.*, **20**, 415—422 (2005).
27) Moellering R. C., Krogstad D. J., Greenblatt D. J., *Rev. Infect. Dis.*, **3S**, S230—S235 (1981).
28) Moise-Broder P. A., Forrest A., Birmingham M. C., Schentag J. J., *Clin. Pharmacokinet.*, **43**, 925—942 (2004).
29) Igarashi M., Nakatani T., Hayashi M., Nakata K., Kasuya Y., *Jpn. J. Chemother.*, **50**, 826—829 (2005). (in Japanese except Abstract)

0022-3565/09/3291-185–191$20.00
THE JOURNAL OF PHARMACOLOGY AND EXPERIMENTAL THERAPEUTICS
Copyright © 2009 by The American Society for Pharmacology and Experimental Therapeutics
JPET 329:185–191, 2009

Vol. 329, No. 1
147918/3454091
Printed in U.S.A.

Involvement of Human Multidrug and Toxin Extrusion 1 in the Drug Interaction between Cimetidine and Metformin in Renal Epithelial Cells

Masahiro Tsuda, Tomohiro Terada, Miki Ueba, Tomoko Sato, Satohiro Masuda, Toshiya Katsura, and Ken-ichi Inui

Department of Pharmacy, Kyoto University Hospital, Faculty of Medicine, Kyoto University, Kyoto, Japan

Received October 24, 2008; accepted January 21, 2009

ABSTRACT

In human proximal tubules, organic cations are taken up from blood into cells by human organic cation transporter 2 [hOCT2/solute carrier (SLC) 22A2] and then eliminated into the lumen by apical H^+/organic cation antiporters, human multidrug and toxin extrusion 1 (hMATE1/SLC47A1) and hMATE2-K (SLC47A2). To evaluate drug interactions of cationic drugs in the secretion process, epithelial cells engineered to express both hOCT2 and hMATE transporters are required to simultaneously evaluate drug interactions with renal basolateral and apical organic cation transporters. In the present study, therefore, we assessed the drug interaction between cimetidine and metformin with double-transfected Madin-Darby canine kidney cells stably expressing both hOCT2 and hMATE1 as an in vitro model of the proximal tubular epithelial cells. The basolateral-to-apical transport and intracellular accumulation of [^{14}C]metformin by a double transfectant were markedly inhibited by 1 mM cimetidine at the basolateral side. On the other hand, 1 μM cimetidine at the basolateral side moderately decreased the basolateral-to-apical transport of [^{14}C]metformin and significantly increased the intracellular accumulation of [^{14}C]metformin from the basolateral side, suggesting that cimetidine at a low concentration inhibits apical hMATE1, rather than basolateral hOCT2. Actually, in concentration-dependent inhibition studies by a single transporter expression system, such as human embryonic kidney 293 stably expressing hMATE1, hMATE2-K, or hOCT2, cimetidine showed higher affinity for hMATEs than for hOCT2. These results suggest that apical hMATE1 is involved in drug interactions between cimetidine and cationic compounds in the proximal tubular epithelial cells.

Drug interactions involving metabolism and/or excretion cause marked changes in plasma and intracellular concentrations of the affected drug. Such interactions can lead to severe adverse effects or unexpected pharmacological effects. Recent studies have shown that many transporters play important roles in the uptake and subsequent secretion of drugs in the liver and kidney, and several specific transporter proteins involved in drug interactions have been reported (Shitara et al., 2005; Endres et al., 2006; Li et al., 2006). However, most of these reports examined the involvement of either apical or basolateral transporters. To reproduce drug interactions via renal transporters in vivo, analyses by the epithelial cells with transcellular transport systems are needed.

This work was supported in part by the Ministry of Health, Labor and Welfare of Japan [Health and Labor Sciences Research Grants]; and the Ministry of Education, Science, Culture and Sports of Japan [Grant-in-aid for Scientific Research].

Article, publication date, and citation information can be found at http://jpet.aspetjournals.org.

doi:10.1124/jpet.108.147918.

In human proximal tubules, organic cations are taken up from blood into cells by human organic cation transporter 2 (hOCT2/SLC22A2) and then eliminated into the lumen by apical H^+/organic cation antiporters, human multidrug and toxin extrusion 1 (hMATE1/SLC47A1) and hMATE2-K (SLC47A2). hMATE1 and hMATE2-K have been identified recently (Otsuka et al., 2005; Masuda et al., 2006), and we have characterized both transporters in terms of tissue distribution, membrane localization, transcriptional regulation, and transport characteristics (Terada and Inui, 2008). However, there has been little systematic comparison of substrate affinity among hMATE1, hMATE2-K, and hOCT2. Comparisons of substrate affinity for hMATEs and hOCT2 would enable us to predict where drug interactions between cationic drugs are likely to occur in the renal secretion process in vivo. It is important to predict where on the membrane drug interaction will occur because the intracellular accumulation of drugs at the proximal tubules may be involved in drug-induced nephrotoxicity.

Here, for a systematic comparison of substrate affinity

ABBREVIATIONS: h, human; OCT, organic cation transporter; SLC, solute carrier; MATE, multidrug and toxin extrusion; MDCK, Madin-Darby canine kidney; TEA, tetraethylammonium; HEK, human embryonic kidney; r, rat.

among hMATE1, hMATE2-K, and hOCT2, the affinity of various drugs for hMATE1 and hMATE2-K was elucidated. Then, based on a comparison of the affinity for the hMATE family and hOCT2, the involvement of hMATE1 in the drug interaction between cimetidine and metformin was evaluated by using double-transfected Madin-Darby canine kidney (MDCK) cells stably expressing both hOCT2 and hMATE1 (MDCK-hOCT2/hMATE1 cells). Recently, we have established this double transfectant, and demonstrated that MDCK-hOCT2/hMATE1 cells are an appropriate in vitro model of human tubular epithelial cells to evaluate the transcellular transport of cationic drugs (Sato et al., 2008).

Materials and Methods

Materials. Pramipexole dihydrochloride monohydrate and talipexole hydrochloride were kindly provided by Nippon Boehringer Ingelheim (Tokyo, Japan). [^{14}C]Tetraethylammonium (TEA) (2.035 GBq/mmol) was purchased from American Radiolabeled Chemicals (St. Louis, MO). [^{14}C]Metformin (962 MBq/mmol) and D-[^{14}C]mannitol (2 GBq/mmol) were purchased from Moravek Biochemicals (Brea, CA). [*N*-Methyl-^{3}H]cimetidine (470 GBq/mmol) was obtained from GE Healthcare (Chalfont St. Giles, UK). D-[1-^{3}H(N)]mannitol (525.4 GBq/mmol) was acquired from PerkinElmer Life and Analytical Sciences (Boston, MA). Quinidine sulfate, verapamil hydrochloride, imipramine hydrochloride, diphenhydramine hydrochloride, (±)-chlorpheniramine maleate, and cimetidine were purchased from Nacalai Tesque (Kyoto, Japan). Metformin hydrochloride, diltiazem hydrochloride, procainamide hydrochloride, ranitidine hydrochloride, and amantadine hydrochloride were obtained from Sigma-Aldrich (St. Louis, MO). Disopyramide, desipramine hydrochloride and famotidine were acquired from Wako Pure Chemicals (Osaka, Japan). Cetirizine was obtained from LKT Labs (St. Paul, MN). All other chemicals used were of the highest purity available.

Cell Culture. According to our previous report (Tanihara et al., 2007), HEK293 cells stably expressing hMATE1 (HEK-hMATE1 cells) or hMATE2-K (HEK-hMATE2-K cells) were cultured in complete medium consisting of Dulbecco's modified Eagle's medium (Sigma-Aldrich) with 10% fetal bovine serum (Invitrogen, Carlsbad, CA) and hygromycin B (0.2 mg/ml; Invitrogen) in an atmosphere of 5% CO_2/95% air at 37°C. The double-transfected MDCK-hOCT2/hMATE1 cells were previously established in our laboratory (Sato et al., 2008). MDCK-hOCT2/hMATE1 cells were cultured in complete medium consisting of Dulbecco's modified Eagle's medium with 10% fetal bovine serum, hygromycin B (0.2 mg/ml), and G-418 (0.5 mg/ml; Nacalai Tesque) in an atmosphere of 5% CO_2/95% air at 37°C. In the previous study, we demonstrated that hOCT2 and hMATE1 were localized on the basolateral and apical membrane, respectively, in MDCK-hOCT2/hMATE1 cells by immunofluorescence microscopy (Sato et al., 2008). HEK293 cells stably expressing hOCT2 (HEK-hOCT2 cells) were cultured according to a previous report (Urakami et al., 2004).

Preparation of Membrane Vesicles from HEK-hMATE1 and HEK-hMATE2-K Cells. HEK-hMATE1 or HEK-hMATE2-K cells were seeded on 100-mm plastic dishes (5×10^6 cells/dish), with 25 dishes used in a single preparation. Then, plasma membrane vesicles were prepared according to our previous report (Tsuda et al., 2007).

Transport Experiments by Membrane Vesicles. The uptake of [^{14}C]TEA by membrane vesicles from HEK-hMATE1 or HEK-hMATE2-K cells was measured using a rapid filtration technique according to our previous report (Tsuda et al., 2007). Nonspecific absorption was determined by the addition of [^{14}C]TEA to 1 ml of ice-cold stop solution containing 20 μl of membrane vesicles. This value was subtracted from the total uptake data. The protein content was determined by the method of Bradford (1976) using a Bio-Rad Protein Assay Kit (Bio-Rad, Hercules, CA) with bovine γ-globulin as a standard.

Transport Experiments by Transfectants. The cellular uptake of radiolabeled compounds was performed as reported previously (Urakami et al., 2004; Tanihara et al., 2007). The transcellular transport experiments with radiolabeled compounds were performed as described previously (Sato et al., 2008). In brief, MDCK-hOCT2/hMATE1 cells were seeded on microporous membrane filters (3.0-μm pores, 4.7-cm^2 growth area) inside a Transwell cell culture chamber (Corning Life Sciences, Lowell, MA) at a density of 18×10^5 cells/well. On the 7th day after the seeding, the cells were used for transcellular transport experiments. The composition of the incubation medium was as follows: 145 mM NaCl, 3 mM KCl, 1 mM $CaCl_2$, 0.5 mM $MgCl_2$, 5 mM D-glucose, and 5 mM HEPES, pH 7.4, or MES, pH 6.0. After the removal of the culture medium from both sides of the monolayers, the cell monolayers were preincubated with 2 ml of incubation medium, pH 7.4, on each side for 10 min at 37°C. Then, 2 ml of incubation medium, pH 7.4, containing both a radiolabeled compound and radiolabeled mannitol was added to the basolateral side, and 2 ml of nonradioactive incubation medium, pH 6.0, was added to the apical side. The monolayers were incubated for specified periods of time at 37°C. Radiolabeled mannitol, a compound that is not transported by the cells, was used to calculate paracellular flux and the extracellular trapping of substrates. For transport measurements, an aliquot (100 μl) of the incubation medium on the apical side was taken at specified times, and the radioactivity was determined in 5 ml of ACSII by liquid scintillation counting. For accumulation studies, the medium was removed by aspiration at the end of the incubation period, and the monolayers were rapidly washed twice with 2 ml of ice-cold incubation medium, pH 7.4, on each side. The filters were detached from the chambers, the cells on the filters were solubilized with 0.5 ml of 0.5 N NaOH, and the radioactivity in aliquots (300 μl) was determined in 3 ml of ACSII by liquid scintillation counting. The protein content of the solubilized cells was determined using a Bio-Rad Protein Assay Kit with bovine γ-globulin as a standard (Bradford, 1976).

Measurement of Intracellular Volume. The equilibrium uptake of sulfanilamide was determined according to standard procedures for transcellular transport experiments with a slight modification. In brief, after the preincubation, 2 ml of incubation medium, pH 7.4, containing both 10 mM sulfanilamide and D-[^{3}H]mannitol was added to both sides. The intracellular volume was calculated from the equilibrium uptake (60 min) and external concentration of sulfanilamide. Sulfanilamide was diazotized and coupled with 2-DEAE-1-naphthylamine oxalate, and the amount of colored material was determined spectrophotometrically at 550 nm (Saito et al., 1986).

Data Analysis. Data were expressed as the means ± S.D. Two or three experiments were conducted, and representative results were shown. Apparent K_i values were expressed as the means ± S.E. and analyzed statistically using the unpaired Student's *t* test. Data from transport experiments were analyzed statistically with the one-way analysis of variance followed by Dunnett's test.

Results

Determination of the Driving Force of hMATE1 and hMATE2-K with Membrane Vesicles from HEK-hMATE1 and HEK-hMATE2-K Cells. At first, to validate the driving force of hMATE1 and hMATE2-K, we carried out [^{14}C]TEA uptake studies with membrane vesicles from HEK-hMATE1 or HEK-hMATE2-K cells. In the presence of an outwardly directed H^+ gradient, a marked stimulation of [^{14}C]TEA uptake (overshoot phenomenon) was observed in membrane vesicles from HEK-hMATE1 and HEK-hMATE2-K cells (Fig. 1, A and B). Furthermore, [^{14}C]TEA uptake by hMATE1 and hMATE2-K was not altered by the presence of valinomycin with or without

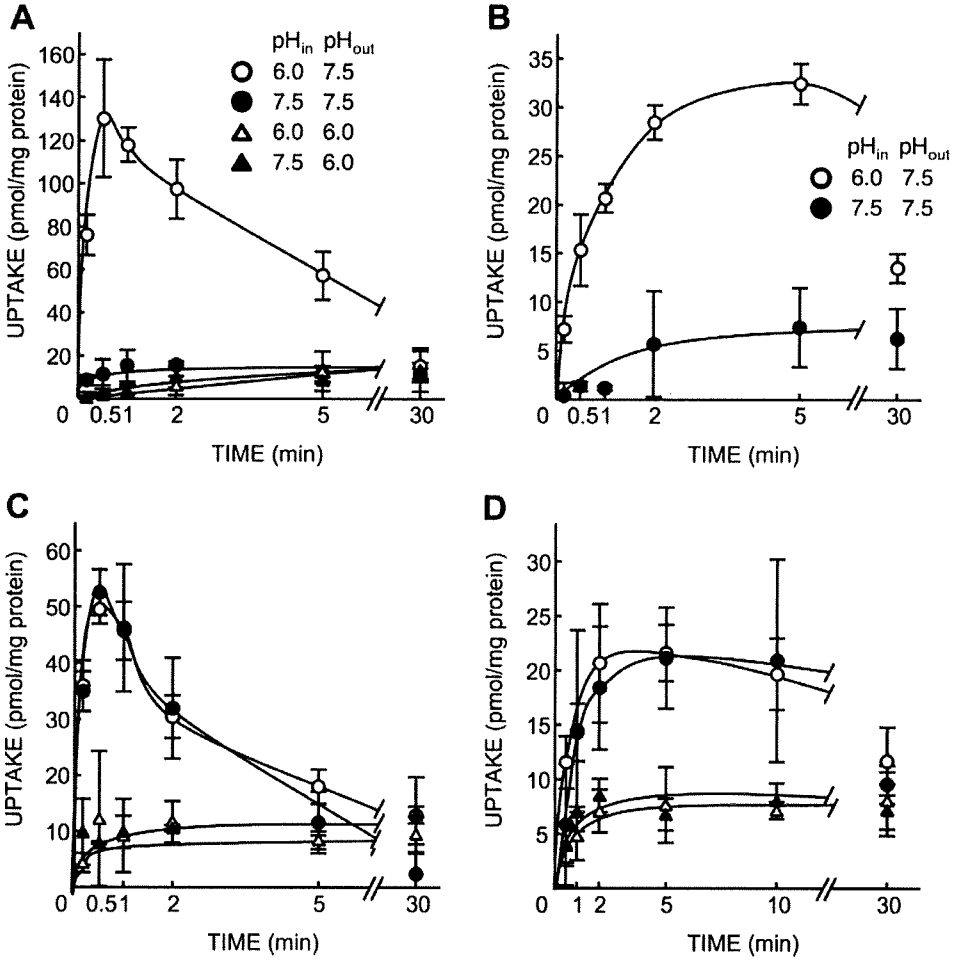

Fig. 1. Determination of the driving force of the hMATE family with membrane vesicles from HEK-hMATE1 (A and C) and HEK-hMATE2-K (B and D) cells. A and B, effects of various H^+ gradients on [^{14}C]TEA uptake. Membrane vesicles were prepared in the experimental buffer at pH 6.0 (○ and △) or 7.5 (● and ▲). The uptake of [^{14}C]TEA was examined in the experimental buffer containing 31.25 μM [^{14}C]TEA and 100 mM KCl at pH 6.0 (△ and ▲) or 7.5 (○ and ●). C and D, effects of valinomycin on [^{14}C]TEA uptake with or without a H^+ gradient. Membrane vesicles were prepared in the experimental buffer at pH 6.0 (○ and ●) or 7.5 (△ and ▲). The uptake of [^{14}C]TEA was examined in the experimental buffer containing 31.25 μM [^{14}C]TEA and 100 mM CsCl at pH 7.5 in the absence (○ and △) or presence (● and ▲) of 8 μM valinomycin. Valinomycin, a K^+ ionophore, was employed to produce an inside-negative membrane potential in the presence of outward K^+ gradient. Each point represents the mean ± S.D. for three determinations. These figures are representative of two separate experiments. pH_{in}, intravesicular pH; pH_{out}, extravesicular pH.

the H^+ gradient (Fig. 1, C and D). These findings indicated that both transporters utilized an oppositely directed H^+ gradient as a driving force. Subsequent experiments were carried out in the presence of an outwardly directed H^+ gradient to evaluate the transport characteristics of the MATE family.

Comparison of Substrate Affinity for hMATE1, hMATE2-K, and hOCT2. To compare the substrate affinity for hMATE1 and hMATE2-K, the apparent K_i values of various cationic drugs for the uptake of [^{14}C]TEA were determined. Cationic drugs inhibited [^{14}C]TEA uptake via hMATE1 and hMATE2-K in a dose-dependent manner. Figures 2 and 3 show representative inhibition curves of histamine H_2 receptor antagonists and antiparkinsonian agents, respectively. Table 1 provides a summary of the apparent K_i values of various drugs for hMATE1 and hMATE2-K. Histamine H_2 receptor antagonists such as cimetidine and famotidine showed high affinity for hMATE1 and hMATE2-K as compared with other drugs. Although many drugs tended to have higher affinity for hMATE1 than for hMATE2-K, only pramipexole, an antiparkinsonian agent, exhibited higher affinity for hMATE2-K than for hMATE1. Table 2 shows the affinity for hMATE1, hMATE2-K, and OCT2 of various compounds excreted from the kidney. K_m values of hOCT2 and rat (r) OCT2 were cited from previous papers (Urakami et al., 2001; Ishiguro et al., 2005; Koepsell et al., 2007). Most drugs showed higher affinity for OCT2 than for hMATEs.

Effects of Cimetidine on Transcellular Transport of [^{14}C]Metformin in MDCK-hOCT2/hMATE1 Cells. It is interesting that histamine H_2 receptor antagonists such as cimetidine showed higher affinity for hMATEs than for hOCT2 (Table 2). Furthermore, recent clinical pharmacokinetic and pharmacogenomic analyses of metformin have paid attention to the renal secretion process (Shikata et al., 2007; Song et al., 2008; Takane et al., 2008; Wang et al., 2008). Therefore, we examined the effect of different concentrations of cimetidine on the basolateral-to-apical transport and intracellular accumulation of [^{14}C]metformin in MDCK-hOCT2/hMATE1 cells. We have demonstrated recently that MDCK-hOCT2/hMATE1 showed the vectorial transcellular transport of organic cations, such as TEA and metformin

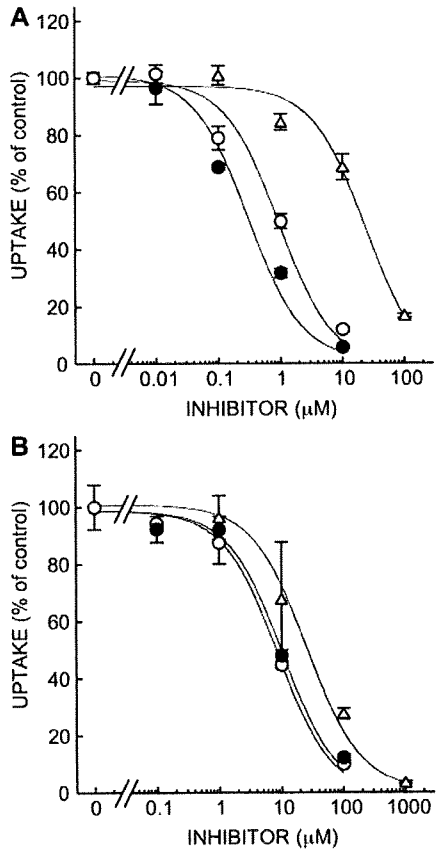

Fig. 2. Effects of histamine H_2 receptor antagonists on [^{14}C]TEA uptake by HEK-hMATE1 (A) and HEK-hMATE2-K (B) cells. HEK-hMATE1 and HEK-hMATE2-K cells were preincubated with 30 mM NH_4Cl, pH 7.4, for 20 min. Then, the preincubation medium was removed, and the cells were incubated with 5 μM [^{14}C]TEA in the presence of cimetidine (○), famotidine (●), or ranitidine (△) for 1 min at 37°C (pH 7.4). After the incubation, the radioactivity of solubilized cells was measured. Each point represents the mean ± S.D. for three monolayers. These figures are representative of three separate experiments.

(Sato et al., 2008). As shown in Fig. 4A, the transcellular transport of [^{14}C]metformin was moderately inhibited by the presence of 1 μM cimetidine and almost completely inhibited by the presence of 1 mM cimetidine. The cellular accumulation of [^{14}C]metformin was inhibited by 1 mM cimetidine but increased by 1 μM cimetidine (Fig. 4B). Furthermore, we examined the inhibitory effects of cimetidine on the uptake of [^{14}C]metformin by hOCT2. Cimetidine had little effect at 1 μM but inhibited the uptake at 1 mM (Fig. 5). The apparent K_i value of cimetidine for hOCT2 was calculated to be 147.1 ± 11.0 μM. These results suggest that 1 mM cimetidine competitively inhibits the uptake of [^{14}C]metformin by hOCT2, resulting in a drastic decrease in both the transcellular transport and the intracellular accumulation of [^{14}C]metformin. On the other hand, 1 μM cimetidine inhibits the apical efflux of [^{14}C]metformin via hMATE1, but not the uptake by hOCT2, causing a marked increase in its cellular accumulation.

Intracellular Concentration of [^{3}H]Cimetidine in MDCK-hOCT2/hMATE1 Cells. To confirm that hMATE1 is specifically inhibited by intracellular cimetidine taken up from the basolateral side, the intracellular concentration of cimetidine was determined. The amount of intracellular cimetidine after 60 min of incubation was demonstrated to be 10.0 ± 0.5 pmol/mg protein. We then measured the intracellular volume of MDCK-hOCT2/hMATE1 cells with the equilibrium uptake of sulfanilamide and found that it was 2.2 ± 0.4 μl/mg protein. Based on these findings, the intracellular concentration of cimetidine was calculated as 4.5 ± 0.4 μM. Considering the K_i values of cimetidine for hMATE1 and hOCT2, this intracellular concentration suggests that the transport of cationic drugs via hMATE1 is specifically inhibited by intracellular cimetidine, but transport via hOCT2 is little inhibited by intracellular cimetidine (Fig. 6).

Discussion

We reported that hMATE1 and hMATE2-K have a similar substrate specificity for many endogenous organic cations and cationic drugs and that several substrates have higher affinity for hMATE1 than for hMATE2-K (Tanihara et al., 2007). In the present study, four cationic drugs had similar affinity for hMATE1 and for hMATE2-K, and 12 cationic drugs were found to have higher affinity for hMATE1 than for hMATE2-K (Table 1). This would suggest that hMATE1 and hMATE2-K have complementary roles in the renal se-

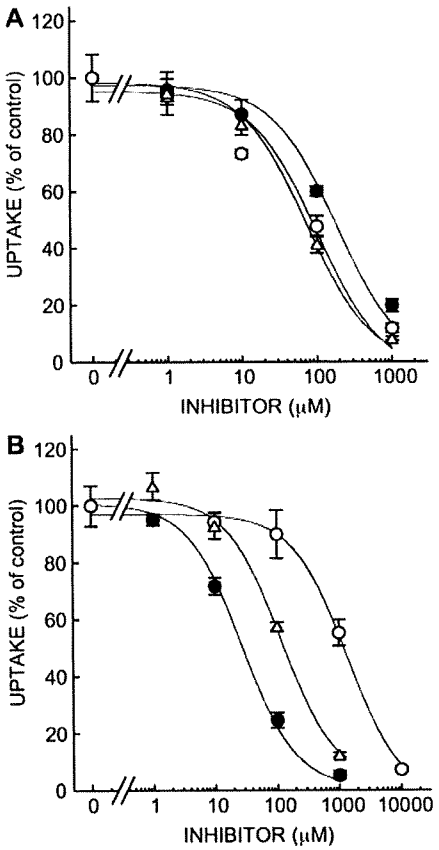

Fig. 3. Effects of antiparkinsonian agents on [^{14}C]TEA uptake by HEK-hMATE1 (A) and HEK-hMATE2-K (B) cells. HEK-hMATE1 and HEK-hMATE2-K cells were preincubated with 30 mM NH_4Cl, pH 7.4, for 20 min. Then, the preincubation medium was removed, and the cells were incubated with 5 μM [^{14}C]TEA in the presence of amantadine (○), pramipexole (●), or talipexole (△) for 1 min at 37°C, pH 7.4. After the incubation, the radioactivity of solubilized cells was measured. Each point represents the mean ± S.D. for three monolayers. These figures are representative of three separate experiments.

TABLE 1
The apparent K_i values of various drugs for [^{14}C]TEA uptake by hMATE1 and hMATE2-K
Each value represents the mean ± S.E. for three independent experiments.

Drug	Apparent K_i Values for [^{14}C]TEA Uptake		Ratio of K_i Values (hMATE1/hMATE2-K)
	hMATE1	hMATE2-K	
	μM		
Antidiabetic drug			
Metformin	666.9 ± 30.2	6515.7 ± 792.4	0.10
Antiarrhythmic drugs			
Diltiazem	12.5 ± 0.7	117.0 ± 2.7*	0.11
Disopyramide	83.8 ± 5.8	291.6 ± 38.3*	0.29
Procainamide	217.0 ± 11.6	178.1 ± 19.3	1.22
Quinidine	29.2 ± 3.1	23.1 ± 4.5	1.26
Verapamil	27.5 ± 3.6	32.1 ± 4.4	0.85
Antidepressant drugs			
Desipramine	55.7 ± 14.5	283.0 ± 53.5*	0.19
Imipramine	42.0 ± 9.0	182.9 ± 31.0*	0.23
Histamine H_1 receptor antagonists			
Cetirizine	371.2 ± 42.7	817.6 ± 103.6*	0.45
Chlorpheniramine	87.6 ± 8.5	191.2 ± 33.6*	0.46
Diphenhydramine	87.0 ± 4.0	266.5 ± 53.4*	0.33
Histamine H_2 receptor antagonists			
Cimetidine	1.1 ± 0.3	7.3 ± 0.7*	0.15
Famotidine	0.6 ± 0.2	9.7 ± 0.4*	0.06
Ranitidine	25.4 ± 2.1	25.0 ± 0.8	1.02
Antiparkinsonian agents			
Amantadine	111.8 ± 5.9	1167.0 ± 100.5*	0.10
Pramipexole	141.4 ± 24.2	24.1 ± 3.4*	5.86
Talipexole	66.0 ± 3.7	119.5 ± 15.3*	0.55

* $P < 0.05$, significantly different from the apparent K_i value of hMATE1.

cretion of organic cations. It is interesting that only pramipexole showed markedly higher affinity for hMATE2-K than for hMATE1 (Fig. 3; Table 1). It has been reported that pramipexole is transported by rOCT1 and rOCT2 (Ishiguro et al., 2005), but it is unclear whether pramipexole is transported by the hMATE family and hOCT2. Pramipexole may be a good probe to distinguish the molecular mechanisms by which the hMATE family recognizes substrates.

In the present study, most drugs showed higher affinity for OCT2 than for hMATEs (Table 2). Histamine H_2 receptor antagonists such as cimetidine and famotidine, however, showed higher affinity for hMATEs than for hOCT2. In particular, the K_i values of cimetidine for hMATE1 and for hOCT2 were 1.1 and 8.6 to 73 μM (Koepsell et al., 2007), respectively. Taking into consideration the effective blood concentration of cimetidine (2.0–3.6 μM) (Benet et al., 1996), it is assumed that hOCT2 is little inhibited by cimetidine at clinical doses, but hMATE1 is inhibited by cimetidine taken up from blood into cells. To verify this hypothesis, we performed transcellular transport studies with a double transfectant composed of basolateral hOCT2 and apical hMATE1. We found that 1 μM cimetidine was taken up from the

TABLE 2
Comparison of affinity for hMATE1, hMATE2-K, and hOCT2 (rOCT2) of organic cations and various drugs excreted from kidney

Compounds	K_m or K_i Values for [^{14}C]TEA Uptake		Affinity for hOCT2 (rOCT2) from Previous Articles[b]	Comparison of Affinity	Effective Plasma Concentration[c]
	hMATE1	hMATE2-K			
	μM				μM
Organic cations					
TEA	380[a]	760[a]	48–270	MATE < OCT	
1-Methyl-4-phenylpyridinium	100[a]	110[a]	19–78	MATE < OCT	
Antidiabetic drug					
Metformin	667	6516	339–1700	MATE < OCT	4.1
Antiarrhythmic drugs					
Disopyramide	84	292	(64)	MATE < OCT	>4.4
Procainamide	217	178	50–58	MATE < OCT	11–52
Quinidine	29	23	(19)	MATE < OCT	6–18
Histamine H_1 receptor antagonist					
Cetirizine	371	818	No data		0.55
Histamine H_2 receptor antagonists					
Cimetidine	1.1	7.3	8.6–73	MATE > OCT	2.0–3.6
Famotidine	0.6	9.7	111–204	MATE > OCT	0.04
Ranitidine	25	25	40–265	MATE > OCT	0.28
Antiparkinsonian agents					
Amantadine	112	1167	20–28	MATE < OCT	1.6
Pramipexole	141	24	(17)	MATE < OCT	0.001
Talipexole	66	120	No data		0.002

[a] The K_m values obtained from a previous paper (Tanihara et al., 2007).
[b] The affinity for OCT2 obtained from previous work (Urakami et al., 2001; Ishiguro et al., 2005; Koepsell et al., 2007).
[c] The effective plasma concentration obtained from the data of Benet et al. (1996).

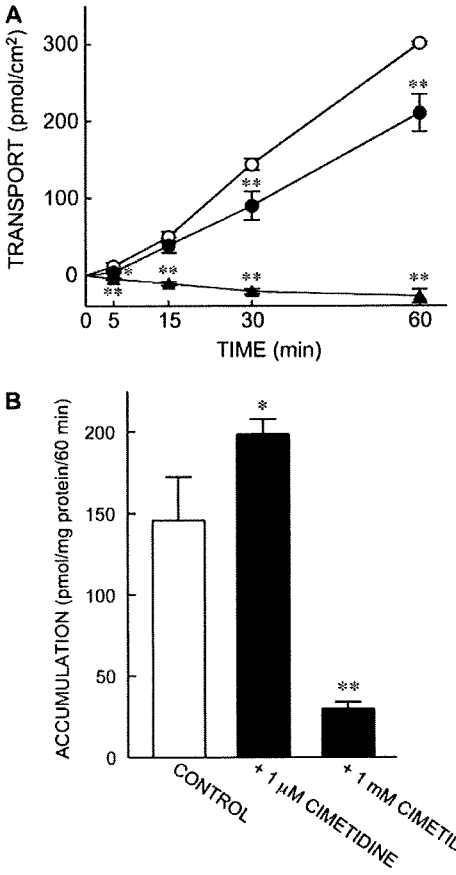

Fig. 4. Effects of cimetidine on transcellular transport (A) and intracellular accumulation (B) of [^{14}C]metformin by MDCK-hOCT2/hMATE1 cells. The cell monolayers were incubated at 37°C with 2 ml of incubation medium, pH 7.4, containing [^{14}C]metformin (10.6 μM) and D-[^{3}H]mannitol (0.079 μM) added to the basolateral side in the absence (Control, ○) or presence of either 1 μM cimetidine (●) or 1 mM cimetidine (▲), and 2 ml of nonradioactive incubation medium, pH 6.0, was added to the apical side. After the incubation, the radioactivity on the apical side and intracellular accumulation were measured. Transcellular transport of [^{14}C]metformin was calculated by subtracting the flux of [^{3}H]mannitol from the net flux of [^{14}C]metformin. After 60 min of incubation, the cell monolayers were washed twice with ice-cold incubation medium, and the radioactivity of solubilized cells was determined. Each point and column represent the mean ± S.D. for three monolayers. When error bars are not shown, they are smaller than the symbols. These figures are representative of two separate experiments. *, $P < 0.05$; **, $P < 0.01$, significantly different from control.

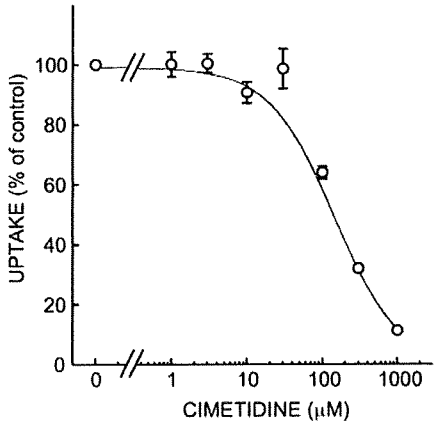

Fig. 5. Effects of cimetidine on [^{14}C]metformin uptake by HEK-hOCT2 cells. HEK-hOCT2 cells were preincubated with incubation medium, pH 7.4, for 10 min. The preincubation medium was removed, and the cells were incubated with 10.6 μM [^{14}C]metformin in the presence of cimetidine for 2 min at 37°C, pH 7.4. The radioactivity of solubilized cells was then measured. Each point represents the mean ± S.D. for three monolayers. This figure is representative of three separate experiments.

basolateral side without an inhibitory effect on metformin transport via hOCT2, and intracellular cimetidine inhibited the transport of metformin via hMATE1 (Figs. 4–6). These results suggest that hMATE1 is responsible for the drug interaction between cimetidine and metformin. In fact, it has been reported that cimetidine significantly increased the area under the curve of metformin by an average of 50% and reduced its renal clearance over 24 h by 27% in human subjects (Somogyi et al., 1987). Cimetidine has been shown to be an inhibitor of the active tubular secretion of many cationic drugs, including procainamide (Somogyi et al., 1983; Christian et al., 1984), *N*-acetylprocainamide (Somogyi et al., 1983), ranitidine (van Crugten et al., 1986), triamterene (Muirhead et al., 1986), pilsicainide (Shiga et al., 2000), and varenicline (Feng et al., 2008). These drug interactions could be partially mediated by hMATE1 at the apical membrane in the proximal tubules.

Recently, it was reported that the 808G>T polymorphism of hOCT2 is associated with a reduced tubular secretion clearance of metformin, and the inhibition by cimetidine also seemed to be dependent on this mutation (Wang et al., 2008). These results suggested that the drug interaction between cimetidine and metformin was affected by accumulation of metformin in the renal epithelial cells. This report would support our notion that the hMATE family plays an important role in the cimetidine-metformin interaction in vivo.

It has been reported that cisplatin, an anticancer platinum agent, was accumulated in the kidney via hOCT2 and induced nephrotoxicity. On the other hand, oxaliplatin was transported by hMATE2-K and hOCT2; therefore, its renal cellular concentration was lowered, suggesting that oxaliplatin did not induce nephrotoxicity (Yonezawa et al., 2006;

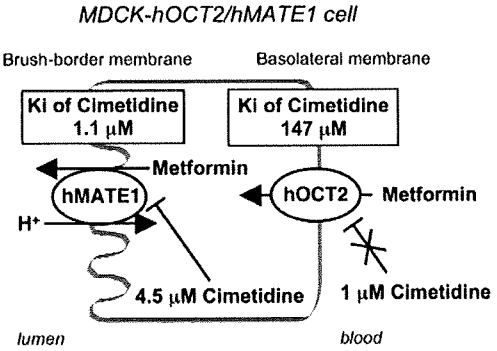

Fig. 6. Scheme of drug interaction between cimetidine and metformin in MDCK-hOCT2/hMATE1 cells. K_i values of cimetidine for hMATE1 and hOCT2 were calculated as 1.1 and 147 μM, respectively. When cimetidine at 1 μM was added to the basolateral side, intracellular concentration of cimetidine after 60 min incubation was calculated as 4.5 ± 0.4 μM. Considering K_i values and intracellular concentration of cimetidine, 1 μM cimetidine at the basolateral side did not inhibit metformin transport via hOCT2. However, intracellular cimetidine at 4.5 μM was enough to inhibit the metformin transport via hMATE1. These findings suggested that apical hMATE1 mainly contributed to the drug interaction between cimetidine and metformin.

Yokoo et al., 2007). The present findings suggested that coadministration of cimetidine may increase the tubular accumulation of oxaliplatin by inhibiting hMATE2-K. Double-transfected MDCK-hOCT2/hMATE1 and MDCK-hOCT2/hMATE2-K cells should be very useful in vitro tools for the screening of renal drug interactions with cationic drugs and nephrotoxicity.

In this study, we clearly demonstrated the driving force of hMATE1 and hMATE2-K to be an oppositely directed H^+ gradient, not inside-negative membrane potential (Fig. 1). These results suggested that [^{14}C]TEA transport via hMATE1 and hMATE2-K is the electroneutral antiport of H^+ and it. The results showed that there was no difference in the driving force between hMATE1 and hMATE2-K and are consistent with a report on transport study with human renal brush-border membrane vesicles (Ott et al., 1990). We also demonstrated previously that [^{14}C]TEA transport by rMATE1 is driven by an oppositely directed H^+ gradient and is electroneutral (Tsuda et al., 2007), suggesting the driving force for the MATE family to be conserved among human and rodents.

In conclusion, we demonstrated for the first time that apical hMATE1 is involved in the drug interaction between cimetidine and metformin in renal epithelial cells. These results provide important information on the physiological and pharmacokinetic roles of the MATE family and may help to avoid the unexpected adverse effects of drug interactions with cationic drugs.

References

Benet L, Oie S, and Schwartz J (1996) Appendices II: design and optimization of dosage regimens; pharmacokinetic data, in *Goodman and Gilman's The Pharmacological Basis of Therapeutics 9th ed* (Hardman J and Limbird L eds) pp 1707–1792, The McGraw-Hill Companies, New York.

Bradford MM (1976) A rapid and sensitive method for the quantitation of microgram quantities of protein utilizing the principle of protein-dye binding. *Anal Biochem* **72:**248–254.

Christian CD Jr, Meredith CG, and Speeg KV Jr (1984) Cimetidine inhibits renal procainamide clearance. *Clin Pharmacol Ther* **36:**221–227.

Endres CJ, Hsiao P, Chung FS, and Unadkat JD (2006) The role of transporters in drug interactions. *Eur J Pharm Sci* **27:**501–517.

Feng B, Obach RS, Burstein AH, Clark DJ, de Morais SM, and Faessel HM (2008) Effect of human renal cationic transporter inhibition on the pharmacokinetics of varenicline, a new therapy for smoking cessation: an in vitro-in vivo study. *Clin Pharmacol Ther* **83:**567–576.

Ishiguro N, Saito A, Yokoyama K, Morikawa M, Igarashi T, and Tamai I (2005) Transport of the dopamine D_2 agonist pramipexole by rat organic cation transporters OCT1 and OCT2 in kidney. *Drug Metab Dispos* **33:**495–499.

Koepsell H, Lips K, and Volk C (2007) Polyspecific organic cation transporters: structure, function, physiological roles, and biopharmaceutical implications. *Pharm Res* **24:**1227–1251.

Li M, Anderson GD, and Wang J (2006) Drug-drug interactions involving membrane transporters in the human kidney. *Expert Opin Drug Metab Toxicol* **2:**505–532.

Masuda S, Terada T, Yonezawa A, Tanihara Y, Kishimoto K, Katsura T, Ogawa O, and Inui K (2006) Identification and functional characterization of a new human kidney-specific H^+/organic cation antiporter, kidney-specific multidrug and toxin extrusion 2. *J Am Soc Nephrol* **17:**2127–2135.

Muirhead MR, Somogyi AA, Rolan PE, and Bochner F (1986) Effect of cimetidine on renal and hepatic drug elimination: studies with triamterene. *Clin Pharmacol Ther* **40:**400–407.

Otsuka M, Matsumoto T, Morimoto R, Arioka S, Omote H, and Moriyama Y (2005) A human transporter protein that mediates the final excretion step for toxic organic cations. *Proc Natl Acad Sci U S A* **102:**17923–17928.

Ott RJ, Hai AC, and Giacomini KM (1990) Mechanisms of interactions between organic anions and the organic cation transporter in renal brush border membrane vesicles. *Biochem Pharmacol* **40:**659–661.

Saito H, Inui K, and Hori R (1986) Mechanisms of gentamicin transport in kidney epithelial cell line (LLC-PK_1). *J Pharmacol Exp Ther* **238:**1071–1076.

Sato T, Masuda S, Yonezawa A, Tanihara Y, Katsura T, and Inui K (2008) Transcellular transport of organic cations in double-transfected MDCK cells expressing human organic cation transporters hOCT1/hMATE1 and hOCT2/hMATE1. *Biochem Pharmacol* **76:**894–903.

Shiga T, Hashiguchi M, Urae A, Kasanuki H, and Rikihisa T (2000) Effect of cimetidine and probenecid on pilsicainide renal clearance in humans. *Clin Pharmacol Ther* **67:**222–228.

Shikata E, Yamamoto R, Takane H, Shigemasa C, Ikeda T, Otsubo K, and Ieiri I (2007) Human organic cation transporter (OCT1 and OCT2) gene polymorphisms and therapeutic effects of metformin. *J Hum Genet* **52:**117–122.

Shitara Y, Sato H, and Sugiyama Y (2005) Evaluation of drug-drug interaction in the hepatobiliary and renal transport of drugs. *Annu Rev Pharmacol Toxicol* **45:**689–723.

Somogyi A, McLean A, and Heinzow B (1983) Cimetidine-procainamide pharmacokinetic interaction in man: evidence of competition for tubular secretion of basic drugs. *Eur J Clin Pharmacol* **25:**339–345.

Somogyi A, Stockley C, Keal J, Rolan P, and Bochner F (1987) Reduction of metformin renal tubular secretion by cimetidine in man. *Br J Clin Pharmacol* **23:**545–551.

Song IS, Shin HJ, Shim EJ, Jung IS, Kim WY, Shon JH, and Shin JG (2008) Genetic variants of the organic cation transporter 2 influence the disposition of metformin. *Clin Pharmacol Ther* **84:**559–562.

Takane H, Shikata E, Otsubo K, Higuchi S, and Ieiri I (2008) Polymorphism in human organic cation transporters and metformin action. *Pharmacogenomics* **9:**415–422.

Tanihara Y, Masuda S, Sato T, Katsura T, Ogawa O, and Inui K (2007) Substrate specificity of MATE1 and MATE2-K, human multidrug and toxin extrusions/H^+-organic cation antiporters. *Biochem Pharmacol* **74:**359–371.

Terada T and Inui K (2008) Physiological and pharmacokinetic roles of H^+/organic cation antiporters (MATE/SLC47A). *Biochem Pharmacol* **75:**1689–1696.

Tsuda M, Terada T, Asaka J, Ueba M, Katsura T, and Inui K (2007) Oppositely directed H^+ gradient functions as a driving force of rat H^+/organic cation antiporter MATE1. *Am J Physiol Renal Physiol* **292:**F593–F598.

Urakami Y, Kimura N, Okuda M, and Inui K (2004) Creatinine transport by basolateral organic cation transporter hOCT2 in the human kidney. *Pharm Res* **21:**976–981.

Urakami Y, Okuda M, Masuda S, Akazawa M, Saito H, and Inui K (2001) Distinct characteristics of organic cation transporters, OCT1 and OCT2, in the basolateral membrane of renal tubules. *Pharm Res* **18:**1528–1534.

van Crugten J, Bochner F, Keal J, and Somogyi A (1986) Selectivity of the cimetidine-induced alterations in the renal handling of organic substrates in humans: studies with anionic, cationic and zwitterionic drugs. *J Pharmacol Exp Ther* **236:**481–487.

Wang ZJ, Yin OQ, Tomlinson B, and Chow MS (2008) OCT2 polymorphisms and in-vivo renal functional consequence: studies with metformin and cimetidine. *Pharmacogenet Genomics* **18:**637–645.

Yokoo S, Yonezawa A, Masuda S, Fukatsu A, Katsura T, and Inui K (2007) Differential contribution of organic cation transporters, OCT2 and MATE1, in platinum agent-induced nephrotoxicity. *Biochem Pharmacol* **74:**477–487.

Yonezawa A, Masuda S, Yokoo S, Katsura T, and Inui K (2006) Cisplatin and oxaliplatin, but not carboplatin and nedaplatin, are substrates for human organic cation transporters (SLC22A1–3 and multidrug and toxin extrusion family). *J Pharmacol Exp Ther* **319:**879–886.

Address correspondence to: Dr. Ken-ichi Inui, Department of Pharmacy, Kyoto University Hospital, Sakyo-ku, Kyoto 606-8507, Japan. E-mail: inui@kuhp.kyoto-u.ac.jp

Drug Metab. Pharmacokinet. 24 (2): 175–179 (2009).

Regular Article

Larger Dosage Required for Everolimus than Sirolimus to Maintain Same Blood Concentration in Two Pancreatic Islet Transplant Patients with Tacrolimus

Eriko SATO[1], Ikuko YANO[1], Masahiro SHIMOMURA[1], Satohiro MASUDA[1], Toshiya KATSURA[1], Shin-ichi MATSUMOTO[2], Teru OKITSU[2], Yasuhiro IWANAGA[2], Shinji UEMOTO[3] and Ken-ichi INUI[1,*]

[1]*Department of Pharmacy, Kyoto University Hospital, Faculty of Medicine, Kyoto University, Kyoto, Japan*
[2]*Transplantation Unit, Kyoto University Hospital, Faculty of Medicine, Kyoto University, Kyoto, Japan*
[3]*Department of Surgery, Graduate School of Medicine, Kyoto University, Kyoto, Japan*

Full text of this paper is available at http://www.jstage.jst.go.jp/browse/dmpk

Summary: We attempted a switch of mammalian target of rapamycin (mTOR) inhibitors from sirolimus to everolimus, a derivative of sirolimus and now on the market in Japan, in two pancreatic islet transplant patients. Both patients were administered tacrolimus with sirolimus or everolimus. They had been administered 5 or 9 mg sirolimus once a day and had maintained a trough concentration of about 15 ng/mL as measured by high performance liquid chromatography with ultraviolet detection. After the switch from sirolimus to everolimus, they were given 10 or 12 mg/day of everolimus twice a day to maintain a trough concentration of 12-15 ng/mL as measured by a fluorescence polarization immunoassay (FPIA) method. Afterward, the blood concentrations of everolimus and sirolimus after the conversion were measured by high performance liquid chromatography with mass spectrometry and everolimus concentrations were found to be 5-10 ng/mL. These data show that a larger dosage is needed for everolimus than sirolimus to maintain the same trough blood concentration. Data obtained by the FPIA for everolimus should be carefully evaluated after switching from sirolimus to everolimus because of the cross-reactivity of the antibody with sirolimus.

Keywords: everolimus; sirolimus; tacrolimus; pancreatic islet transplantation

Introduction

Pancreatic islet transplantation is a critical treatment for type 1 diabetes when it is difficult to control blood glucose levels despite an optimal insulin regimen and less invasive than pancreatic transplantation. With the Edmonton protocol,[1)] results of pancreatic islet transplantation improved markedly. According to the Edmonton protocol, Kyoto University Hospital performed 17 transplantations from non-heart-beating donors for 9 patients as of the end of 2006. The first successful living-donor islet transplantation was carried out on January 19, 2005.[2)]

The Edmonton protocol consists of high-dose sirolimus (rapamycin) and low-dose tacrolimus for immunosuppression.[1)] Sirolimus suppresses the proliferation of lymphocytes by blocking growth factor-driven signal transduction through the inhibition of mammalian target of rapamycin (mTOR).[3)] In Japan, however, sirolimus is not approved by the Japanese government as an immunosuppressant. Everolimus, a derivative of sirolimus, has a shorter elimination half-life than sirolimus,[4-6)] and is expected to achieve a steady-state more quickly and adjust blood concentrations more easily. Everolimus has already been approved as an immunosuppressant in Europe and in March 2007, was approved as an immunosuppressant for heart transplant patients in Japan. Hence, we conducted a switch of mTOR inhibitors from sirolimus to everolimus in pancreatic islet transplant patients. Generally, clinical studies on everolimus in organ transplant patients have been performed with the concomitant administration of cyclosporine and steroids. There are a few reports on everolimus using tacrolimus.

Received; August 6, 2008, Accepted; November 12, 2008
**To whom correspondence should be addressed;* Ken-ichi INUI, PhD, *Department of Pharmacy, Kyoto University Hospital, Sakyo-ku, Kyoto 606-8507, Japan. Tel. +81-75-751-3577, Fax. +81-75-751-4207, Email: inui@kuhp.kyoto-u.ac.jp*
This work was supported in part by a Grant-in-Aid from the Japan Health Sciences Foundation, by a Grant-in-aid for Scientific Research from the Ministry of Education, Culture, Sports, Science and Technology of Japan, by the 21st Century COE Program 'Knowledge Information Infrastructure for Genome Science', and by a Grant-in-Aid from the Uehara Memorial Foundation. M. S. was supported as a Research Fellow by the 21st Century COE program 'Knowledge Information Infrastructure for Genome Science'.

Since everolimus as well as cyclosporine and tacrolimus are metabolized by cytochrome P450 (CYP) 3A and also transported via P-glycoprotein,[7-9] pharmacokinetic interactions may vary between everolimus and tacrolimus or cyclosporine.

Here, we report pharmacokinetic differences between sirolimus and everolimus in two pancreatic islet transplant patients concomitantly administered tacrolimus. The blood concentration of everolimus was measured by fluorescence polarization immunoassay (FPIA) method as well as high performance liquid chromatography with mass spectrometry (LC/MS).

Methods

Ethics: These studies were conducted in accordance with the Declaration of Helsinki and its amendments and were approved by the Kyoto University Graduate School and Faculty of Medicine Ethics Committee. Written informed consent was obtained from each patient.

Monitoring of blood concentrations for immunosuppressants: Whole blood concentrations of sirolimus (Rapamune®, Wyeth, Madison, NJ) were measured by high performance liquid chromatography with ultraviolet detection (HPLC-UV) as described previously.[10] The whole blood concentration of everolimus (Certican®, Novartis Pharma AG, Basel, Switzerland) was determined by a FPIA (Innofluor® Certican® Assay, Seradyn, Inc., Indianapolis, IN) using a TDxFLx® analyzer (Abbott Japan Co. Ltd., Tokyo, Japan).

Remnant blood samples after measurement of everolimus by FPIA were stored at −80°C. Everolimus and sirolimus whole blood concentrations were determined by a liquid-liquid extraction procedure and analysis of the extract by LC/MS in selected ion monitoring mode using atmospheric pressure chemical ionization as an interface at the laboratory of Novartis Pharma S. A. S. (Rueil Malmaison, France). Assay quantification limits were 0.3 ng/mL for everolimus and 0.5 ng/mL for sirolimus.

Cross-reactivity of sirolimus with the antibody for everolimus: To evaluate the cross-reactivity of sirolimus with the antibody for everolimus used in the assay, sirolimus was spiked in control human whole blood and sirolimus concentration was measured using FPIA for everolimus. Sirolimus concentrations were prepared at 5, 10, 20 and 50 ng/mL and tested in triplicate.

Time course study of everolimus in islet transplant patients: On the day immediately before the discharge of each patient, a time course study of everolimus was conducted. Blood samples were collected just before and 1, 2, 4, and 8 hrs after the morning administration. Whole blood concentrations of everolimus were determined using LC/MS at the laboratory of Novartis.

Results

Case report: Patient 1, a 48-year-old Japanese woman, had been treated with sirolimus and tacrolimus (Prograf®, Astellas Pharma Inc., Tokyo, Japan) after islet transplantation, according to the Edmonton protocol.[1] Thirty-six days after the transplantation, the mTOR inhibitor was converted. We called the day of conversion day 0. Both everolimus and sirolimus were administered on day 0 and only everolimus was administered after that. She kept taking tacrolimus as before (3–4 mg/day). Sirolimus was administered once a day. Everolimus and tacrolimus were administered twice daily. Blood sampling was performed once a day in the morning before the next administration of drugs. Before day 0, the whole blood concentration of sirolimus was quantified by HPLC-UV to adjust the trough concentration of sirolimus to 12–15 ng/mL. After day 0, the dosage of everolimus was adjusted to achieve a target trough blood concentration of 12–15 ng/mL as determined by FPIA. On day 0, the administration of everolimus was started at 4 mg/day, which was less than the dosage of sirolimus on day −1 (5 mg/day). Since the trough concentration of everolimus gradually decreased, the everolimus dosage was increased to 10 mg/day and the blood concentration reached the target level (**Fig. 1**, upper panel).

Patient 2, a 41-year-old Japanese woman, started the administration of everolimus 63 days after transplantation. Based on experience with patient 1, from the start, she was administered 12 mg/day of everolimus, this being greater than the dosage of sirolimus on day −1 (9 mg/day). As a result she did not experience a remarkable fall in the trough concentration of everolimus (**Fig. 1**, lower panel). During the switch from sirolimus to everolimus, she was concomitantly administered 4–6 mg/day of tacrolimus.

Neither patient showed remarkable change in tacrolimus trough concentration, which remained at 3–6 ng/mL, or had clinical complications during the study period. Neither patient was treated with potent inducers or inhibitors of CYP3A and P-glycoprotein.

Pharmacokinetic analysis: Whole blood concentrations of everolimus and sirolimus after the conversion were determined using LC/MS. After discontinuance of administration, sirolimus remained in the blood for several days (**Fig. 1**). The concentration of everolimus measured by FPIA was greater than that obtained by LC/MS, especially immediately after the conversion. To evaluate the cross-reactivity of sirolimus with the antibody for everolimus in the assay, we measured concentrations of sirolimus spiked in control human whole blood using FPIA for everolimus. As shown in **Figure 2**, the antibody for everolimus showed extensive cross-reactivity with sirolimus ([Detected as everolimus] = 1.43 + 0.47 × [Sirolimus concentration], $r^2 = 0.992$).

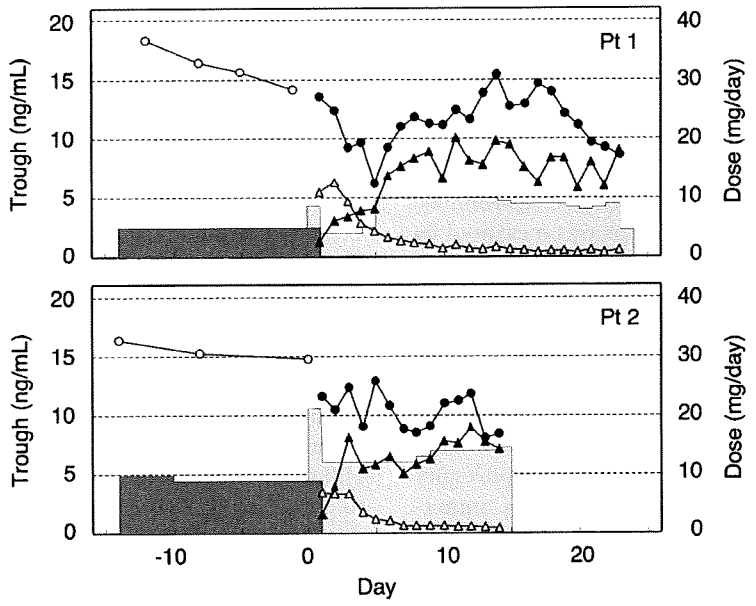

Fig. 1. Trough blood concentrations of sirolimus measured by HPLC-UV (open circles) and LC-MS (open triangles) and those of everolimus measured by FPIA (closed circles) and LC-MS (closed triangles) are plotted for each patient
Dark and light shaded areas show daily dosages of sirolimus and everolimus, respectively.

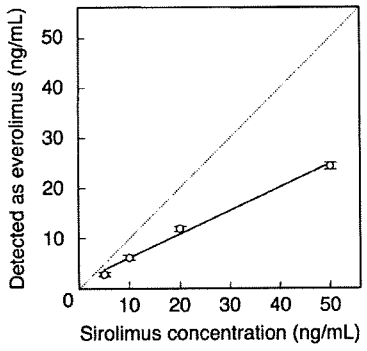

Fig. 2. Sirolimus blood concentrations measured by the FPIA method for everolimus. Each point represents the mean ± SD (n = 3)
The solid line shows the fitting line. The dotted line represents the line of identity (*i.e.*, slope = 1).

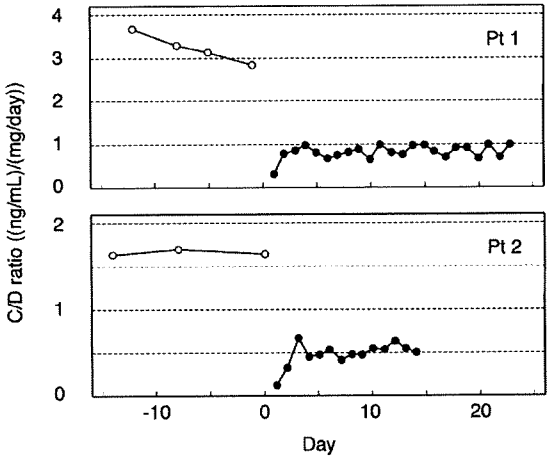

Fig. 3. The trough concentration per dose (C/D) ratios of sirolimus (open circles) and everolimus (closed circles) were plotted for each patient

Figure 3 shows the trough concentration per dose (C/D) ratio profiles of sirolimus and everolimus. C/D ratios of everolimus were calculated from concentrations determined by LC/MS and the dosage administered on the previous day. In patient 1, C/D ratios of sirolimus and everolimus were 3.26 ± 0.35 (ng/mL)/(mg/day) (mean ± standard deviation, n = 4) and 0.87 ± 0.12 (n = 22, except day 1), respectively. In patient 2, the ratios were 1.67 ± 0.03 (n = 3) and 0.52 ± 0.09 (n = 13, except day 1), respectively. In each patient, the C/D ratio of everolimus was approximately three times less that of sirolimus. C/D ratios of everolimus and sirolimus in patient 1 were twice those in patient 2.

We performed a time course study on everolimus. On day 23 for patient 1 and day 13 for patient 2. Everolimus concentration profiles measured by LC/MS are shown in **Figure 4**. Patient 1 was administered 4.5 mg everolimus and the peak concentration (17.1 ng/mL) was obtained at

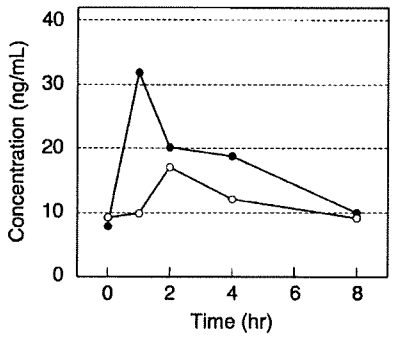

Fig. 4. Everolimus blood concentration profiles after oral administration in the two patients
Open and closed circles show everolimus concentration of patient 1 and patient 2, respectively.

2 h after the administration. Patient 2 was administered 7 mg everolimus and the peak concentration (31.8 ng/mL) was obtained at 1 h. The areas under the concentratioin-time curve from 0 to 8 h (AUC_{0-8}) calculated by the trapezoidal method were 94 and 142 ng·hr/mL in patient 1 and patient 2, respectively, while the concentrations at pre-dose and 8 h in patient 1 were nearly the same as those in patient 2, respectively.

Discussion

As shown in **Figure 1**, our patients were administered 8–14 mg/day of everolimus (with tacrolimus), and achieved trough concentrations of 5–10 ng/mL as measured by the LC/MS. Compared with other reports in which 1.5 or 3 mg/day of everolimus with cyclosporine were administered to renal transplant patients to maintain trough concentrations in a similar range,[11,12] our doses were quite large. We consider that this discrepancy mainly resulted from the difference in calcineurin inhibitor used, namely tacrolimus or cyclosporine. Everolimus as well as tacrolimus and cyclosporine are substrates of CYP3A and P-glycoprotein,[7–9] but lower blood concentrations of tacrolimus than cyclosporine in the clinical situation compared with each affinity value may have little influence on the pharmacokinetics of everolimus. Recently, Kovarik *et al.*[13] reported that the level of exposure to everolimus was 2.5 fold higher with cyclosporine than tacrolimus. It has been reported that average everolimus predose blood concentrations were significantly lower by 2.9 fold in the absence compared with the presence of cyclosporine.[12] The trough concentrations of sirolimus with cyclosporine are reported to be 1.42 times higher than those with tacrolimus.[14] Taking these findings into consideration, cyclosporine has a more profound effect on everolimus than sirolimus pharmacokinetics and our patients may need a considerably larger dosage of everolimus due to the lack of pharmacokinetic interaction with tacrolimus.

Interestingly, the C/D ratio of everolimus was three times smaller than that of sirolimus in the same patients (**Fig. 3**). Coadministration of inhibitors or inducers of CYP3A or P-glycoprorein would be expected to alter sirolimus or everolimus pharmacokinetics, but comedications in the two patients did not change during the study period. Hepatic impairment would decrease the oral clearance of sirolimus,[15] but neither patient had clinical complications such as hepatic dysfunction. Actually, the trough concentrations of tacrolimus, also metabolized by CYP3A and transported via P-glycoprotein, remained in a similar range during the conversion from sirolimus to everolimus in these patients. Therefore, we consider that a larger dosage is needed for everolimus than sirolimus to maintain the same trough blood concentration in the same patients with tacrolimus. As discussed in the previous paragraph, in the case of concomitant administration of cyclosporine, dosage of everolimus might not be so different from that of sirolimus, because of the more profound pharmacokinetic interaction of cyclosporine with everolimus compared to sirolimus. Pharmacokinetic differences between sirolimus and everolimus with cyclosporine in the same patient should be clarified in future study.

Everolimus has been reported to have a large inter-individual variability in the pharmacokinetics,[16] as also found in our cases. In the time course study, the trough concentrations of everolimus in patients 1 and 2 were similar and peak concentrations and AUC_{0-8} in patient 2 were approximately twice those in patient 1 at dosage of 7 mg and 4.5 mg, respectively (**Fig. 4**). Apparent clearance of everolimus approximately estimated by the dose-normalized AUC_{0-8} seems similar in these patients. In contrast, dose-normalized trough concentrations for everolimus and sirolimus were different as also shown in **Figure 3**. One possible reason for these findings is that the patients had different absorption profiles. In general, the recommended therapeutic range for everolimus is reported as a trough concentration of 3 to 8 ng/mL[17] and the clinical significance of AUC monitoring for everolimus remains to be elucidated.

FPIA is easy and convenient to determine whole blood concentrations of everolimus, but it is known to overestimate everolimus concentrations due to cross-reactivity of the antibody with metabolites of everolimus.[18] Actually, the everolimus concentration measured by FPIA was greater than that obtained by LC/MS over the study period (**Fig. 1**). This finding is consistent with a report using samples from renal transplant recipients.[19] In a recent report,[20] FPIA gave a positive bias of 1.2 ng/mL compared with HPLC-UV. The antibody for everolimus may cross-react with sirolimus because of the similarity in chemical structure between everolimus and sirolimus. Immediately after switching of the mTOR inhibitors, it was considered that few metabolites of everolimus were present in blood, but the values obtained were greater

with FPIA than LC/MS (**Fig. 1**). We consider the difference between the two methods to be caused by cross-reactivity with sirolimus and clarified the cross-reactivity of sirolimus with the antibody used in FPIA for everolimus (**Fig. 2**), as consistent with recent reports.[19,20] However, since the values measured by FPIA exceeded the sum of everolimus and sirolimus concentrations measured by LC/MS immediately after the conversion (**Fig. 1**), we consider that metabolites of sirolimus may also cross-react with the antibody of FPIA. These results indicate that the values of everolimus by the FPIA method should be carefully evaluated especially when transplant patients are switched from sirolimus to everolimus.

In conclusion, we report two cases of changing mTOR inhibitors from sirolimus to everolimus with tacrolimus after pancreatic islet transplantation. Each patient needed a considerably larger dosage of everolimus compared to sirolimus to maintain the same trough blood concentrations, which may be explained by lack of pharmacokinetic interaction between tacrolimus and mTOR inhibitors. The concentrations of everolimus measured by FPIA were considerably greater than those by LC/MS. These findings should provide useful information regarding the replacement of sirolimus with everolimus in transplant patients.

References

1) Shapiro, A. M., Lakey, J. R., Ryan, E. A., Korbutt, G. S., Toth, E., Warnock, G. L., Kneteman, N. M. and Rajotte, R. V.: Islet transplantation in seven patients with type 1 diabetes mellitus using a glucocorticoid-free immunosuppressive regimen. *N. Engl. J. Med.*, **343**: 230–238 (2000).
2) Matsumoto, S., Okitsu, T., Iwanaga, Y., Noguchi, H., Nagata, H., Yonekawa, Y., Yamada, Y., Fukuda, K., Tsukiyama, K., Suzuki, H., Kawasaki, Y., Shimodaira, M., Matsuoka, K., Shibata, T., Kasai, Y., Maekawa, T., Shapiro, J. and Tanaka, K.: Insulin independence after living-donor distal pancreatectomy and islet allotransplantation. *Lancet*, **365**: 1642–1644 (2005).
3) Neuhaus, P., Klupp, J. and Langrehr, J. M.: mTOR inhibitors: an overview. *Liver Transpl.*, **7**: 473–484 (2001).
4) Crowe, A., Bruelisauer, A., Duerr, L., Guntz, P. and Lemaire, M.: Absorption and intestinal metabolism of SDZ-RAD and rapamycin in rats. *Drug Metab. Dispos.*, **7**: 627–632 (1999).
5) Kovarik, J. M., Kalbag, J., Figueiredo, J., Rouilly, M., Frazier, O. L. and Rordorf, C.: Differential influence of two cyclosporine formulations on everolimus pharmacokinetics: a clinically relevant pharmacokinetic interaction. *J. Clin. Pharmacol.*, **42**: 95–99 (2002).
6) Zimmerman, J. J., Harper, D., Getsy, J. and Jusko, W. J.: Pharmacokinetic interactions between sirolimus and microemulsion cyclosporine when orally administered jointly and 4 hours apart in healthy volunteers. *J. Clin. Pharmacol.*, **43**: 1168–1176 (2003).
7) Jacobsen, W., Serkova, N., Hausen, B., Morris, R. E., Benet, L. Z. and Christians, U.: Comparison of the in vitro metabolism of the macrolide immunosuppressants sirolimus and RAD. *Transplant. Proc.*, **33**: 514–515 (2001).
8) Crowe, A. and Lemaire, M.: In vitro and in situ absorption of SDZ-RAD using a human intestinal cell line (Caco-2) and a single pass perfusion model in rats: comparison with rapamycin. *Pharm. Res.*, **15**: 1666–1672 (1998).
9) Hebert, M. F.: Contributions of hepatic and intestinal metabolism and P-glycoprotein to cyclosporine and tacrolimus oral drug delivery. *Adv. Drug Deliv. Rev.*, **27**: 201–214 (1997).
10) Sato, E., Shimomura, M., Masuda, S., Yano, I., Katsura, T., Matsumoto, S., Okitsu, T., Iwanaga, Y., Noguchi, H., Nagata, H., Yonekawa, Y. and Inui, K.: Temporal decline in sirolimus elimination immediately after pancreatic islet transplantation. *Drug Metab. Pharmacokinet.*, **21**: 492–500 (2006).
11) Kovarik, J. M., Kaplan, B., Silva, H. T., Kahan, B. D., Dantal, J., McMahon, L., Berthier, S., Hsu, C. H. and Rordorf, C.: Pharmacokinetics of an everolimus-cyclosporine immunosuppressive regimen over the first 6 months after kidney transplantation. *Am. J. Transplant.*, **3**: 606–613 (2003).
12) Kovarik, J. M., Dantal, J., Civati, G., Rizzo, G., Rouilly, M., Betoni-Ristic, O. and Rordorf, C.: Influence of delayed initiation of cyclosporine on everolimus pharmacokinetics in de novo renal transplant patients. *Am. J. Transplant.*, **3**: 1576–1580 (2003).
13) Kovarik, J. M., Curtis, J. J., Hricik, D. E., Pescovitz, M. D., Scantlebury, V. and Vasquez, A.: Differential pharmacokinetic interaction of tacrolimus and cyclosporine on everolimus. *Transplant. Proc.*, **38**: 3456–3458 (2006).
14) Wu, F. L., Tsai, M. K., Chen, R. R., Sun, S. W., Huang, J. D., Hu, R. H., Chen, K. H. and Lee, P. H.: Effects of calcineurin inhibitors on sirolimus pharmacokinetics during staggered administration in renal transplant recipients. *Pharmacotherapy*, **25**: 646–653 (2005).
15) Zimmerman, J. J., Lasseter, K. C., Lim, H. K., Harper, D., Dilzer, S. C., Parker, V. and Matschke, K.: Pharmacokinetics of sirolimus (rapamycin) in subjects with mild to moderate hepatic impairment. *J. Clin. Pharmacol.*, **45**: 1363–1372 (2005).
16) Kovarik, J. M., Kahan, B. D., Kaplan, B., Lorber, M., Winkler, M., Rouilly, M., Gerbeau, C., Cambon, N., Boger, R. and Rordorf, C. on behalf of the Everolimus Phase 2 Study Group.: Longitudinal assessment of everolimus in de novo renal transplant recipients over the first post-transplant year: pharmacokinetics, exposure-response relationships, and influence on cyclosporine. *Clin. Pharmacol. Ther.*, **69**: 48–56 (2001).
17) Mabasa, V. H. and Ensom, M. H.: The role of therapeutic monitoring of everolimus in solid organ transplantation. *Ther. Drug Monit.*, **27**: 666–676 (2005).
18) Strom, T., Haschke, M., Boyd, J., Roberts, M., Arabshahi, L., Marbach, P. and Christians, U.: Crossreactivity of isolated everolimus metabolites with the Innofluor Certican immunoassay for therapeutic drug monitoring of everolimus. *Ther. Drug Monit.*, **29**: 743–749 (2007).
19) Salm, P., Warnholtz, C., Boyd, J., Arabshahi, L., Marbach, P. and Taylor, P. J.: Evaluation of a fluorescent polarization immunoassay for whole blood everolimus determination using samples from renal transplant recipients. *Clin. Biochem.*, **39**: 732–738 (2006).
20) Khoschsorur, G., Fruehwirth, F., Zelzer, S., Stettin, M. and Halwachs-Baumann, G.: Comparison of fluorescent polarization immunoassay (FPIA) versus HPLC to measure everolimus blood concentrations in clinical transplantation. *Clin. Chim. Acta.*, **380**: 217–221 (2007).

Biochemical Pharmacology 78 (2009) 1263–1271

Contents lists available at ScienceDirect

Biochemical Pharmacology

journal homepage: www.elsevier.com/locate/biochempharm

Protective effect of concomitant administration of imatinib on cisplatin-induced nephrotoxicity focusing on renal organic cation transporter OCT2

Yuko Tanihara, Satohiro Masuda, Toshiya Katsura, Ken-ichi Inui *

Department of Pharmacy, Kyoto University Hospital, Faculty of Medicine, Kyoto University, Sakyo-ku, Kyoto 606-8507, Japan

ARTICLE INFO

Article history:
Received 19 April 2009
Accepted 10 June 2009

Keywords:
Chemotherapy
Cisplatin
Imatinib
OCT
MATE
Nephrotoxicity

ABSTRACT

Although the organic cation transporter 2 (OCT2/SLC22A2) mediate renal tubular uptake of cisplatin from the circulation, neither apical multidrug and extrusion (MATE) 1 or MATE2-K mediate tubular secretion of the agent. Therefore, the highly concentrated tubular cisplatin potentiates nephrotoxicity, and these are considered to be a critical mechanism for cisplatin-induced nephrotoxicity. In the present study, we examined the protective effect of imatinib, a cationic anticancer agent, on that nephrotoxicity. Imatinib markedly reduced cisplatin-induced cytotoxicity and platinum accumulation in OCT2-expressing HEK293 cells, but almost no change was found in the cells expressing human MATE1, MATE2-K and rat MATE1. In rats, the renal accumulation of platinum and subsequent nephrotoxicity, based on the blood urea nitrogen, plasma creatinine and creatinine clearance, were significantly decreased with the oral administration of imatinib. The orally administered imatinib significantly increased the area under the plasma concentration–time curve of intravenously administered cisplatin for 3 min by an average of 120%. In additional, the concomitant administration of imatinib clearly avoided the severe renal impairment by the histological examination. In conclusion, the concomitant administration of imatinib with cisplatin prevents cisplatin-induced nephrotoxicity inhibiting the OCT2-mediated renal accumulation of cisplatin.

1. Introduction

Although Cis-diamminedichloroplatinum II (cisplatin, CDDP) is widely used against malignant solid tumors [1,2], severe nephrotoxicity limits its clinical application [3]. Recently, the renal organic cation transporter OCT2-mediated renal accumulation of cisplatin was found to be a key mechanism for its nephrotoxicity both in rats and humans [4,5].

Imatinib (STI-571), a potent inhibitor of ABL tyrosine kinase, has been used for the treatment of Philadelphia chromosome-positive (Ph^+) chronic myeloid leukemia (CML) and Ph^+ acute lymphoblastic leukemia (ALL) [6,7]. Previous studies have suggested that leukocytic hOCT1 mediated the uptake of imatinib and this expression was an important clinical determinant of the pharmacological response of imatinib in CML patients [8–11]. Based on these reports, imatinib might interact with other members of organic cation transporters, such as OCT2, MATE1 (multidrug and toxin extrusion) and MATE2-K [12,13], in addition to OCT1.

In the present study, we hypothesized and examined that the concomitant administration of imatinib prevents cisplatin-induced nephrotoxicity, mainly based on the inhibition of OCT2-mediated renal accumulation of cisplatin, using transporter-expressing cells and rat.

2. Materials and methods

2.1. Materials

Cisplatin was obtained from Sigma Chemical Co. (St. Louis, MO). Imatinib was a kindly gift from Novartis Pharma AG (Basel, Switzerland). NaCl, KCl, $CaCl_2$, $MgCl_2$, D-glucose, HEPES, NaOH, and dimethylsulfoxide were obtained from Nacalai Tesque (Kyoto, Japan). Ammonium chloride and Triton X-100 were obtained from Wako Pure Chemical Industries (Osaka, Japan).

2.2. Cell culture and transfection

Human embryonic kidney (HEK) 293 cells (American Type Culture Collection CRL-1573, Manassas, VA) were cultured in complete medium consisting of Dulbecco's modified Eagle's

Abbreviation: cisplatin, Cis-diamminedichloroplatinum II; hOCT, human organic cation transporter; rOCT, rat organic cation transporter; hMATE, human multidrug and toxin extrusion; rMATE, rat multidrug and toxin extrusion; HEK, human embryonic kidney; ICP-MS, inductively coupled plasma-mass spectrometry; LDH, lactate dehydrogenase.

* Corresponding author. Tel.: +81 75 751 3577; fax: +81 75 751 4207.
E-mail address: inui@kuhp.kyoto-u.ac.jp (K.-i. Inui).

0006-2952/$ – see front matter © 2009 Published by Elsevier Inc.
doi:10.1016/j.bcp.2009.06.014

medium (Sigma) with 10% fetal bovine serum (Invitrogen, Carlsbad, CA) in an atmosphere of 5% CO_2/95% air at 37 °C, and used as host cells. pCMV6-XL4 plasmid vector DNA (OriGene Technologies, Rockville, MD), pBK-CMV plasmid vector DNA (Stratagene, La Jolla, CA) or pcDNA3.1/Hygro(+) plasmid vector DNA (Invitrogen) containing hOCT1, hOCT2, hOCT2-A, rOCT1, rOCT2, hMATE1, hMATE2-K, and rMATE1 cDNAs were used to conduct the transient expression analysis. For transient expression systems, HEK293 cells were transfected with each cDNA or empty vector using LipofectAMINE 2000 Reagent® (Invitrogen) according to the manufacturer's instructions. At 48 h after transfection, the cells were used for uptake experiments.

2.3. Uptake experiments

Cellular uptake of [^{14}C]creatinine (2.035 GBq/mmol; American Radiolabeled Chemicals Inc., St. Louis, MO) was measured with cultures of HEK293 cells grown on poly-D-lysine-coated 24-well plates (Becton, Dickinson and Company, Tokyo, Japan). Typically, the cells were preincubated with 0.2 mL incubation medium (145 mM NaCl, 3 mM KCl, 1 mM $CaCl_2$, 0.5 mM $MgCl_2$, 5 mM D-glucose, 5 mM HEPES, pH 7.4) for 10 min at 37 °C. The medium was then removed, and 0.2 mL incubation medium containing radiolabeled substrate was added. The medium was aspirated off at the end of incubation, and the monolayers were rapidly rinsed three times with 1 mL ice-cold incubation medium. The cells were solubilized in 0.5 mL of 0.5 N NaOH, and then the radioactivity in aliquots was determined by liquid scintillation counting. To manipulate the intracellular pH, intracellular acidification was performed by pretreatment in incubation medium with ammonium chloride (30 mM, 20 min at 37 °C, pH 7.4).

The accumulation of cisplatin was measured using monolayer cultures of HEK293 cells seeded on poly-D-lysine-coated 24-well plates. Both cisplatin and/or imatinib were dissolved with 0.5% dimethylsulfoxide to the final concentration in the treatment medium. After removal of the culture medium, 0.5 mL Dulbecco's modified Eagle's medium with 10% fetal bovine serum containing cisplatin with or without imatinib was added and the monolayers were incubated for 2 h in an atmosphere of 5% CO_2/95% air at 37 °C. After this incubation, the monolayers were rapidly washed twice with ice-cold incubation buffer containing 3% bovine serum albumin (Nacalai Tesque) and then washed three times with ice-cold incubation buffer. The cells were solubilized in 0.5N NaOH, and the amount of platinum was determined using inductively coupled plasma-mass spectrometry (ICP-MS) by the Pharmacokinetics and Bioanalysis Center, Shin Nippon Biomedical Laboratories, Ltd. (Wakayama, Japan).

The protein content of the solubilized cells was determined using a Bio-Rad Protein Assay Kit (Bio-Rad Laboratories, Hercules, CA) with bovine γ-globulin as a standard.

2.4. Measurement of cytotoxicity

The cytotoxicity of the platinum agents was measured with HEK293 cells seeded on poly-D-lysine-coated 24-well plates. Cells were incubated with medium containing cisplatin with or without imatinib or corticosterone (Sigma) for 2 h. After removal of the medium, a drug-free medium was added. After incubation for 24 h, the medium was collected, and the lactate dehydrogenase (LDH) activity and caspase-3 and -7 activities in the medium were measured using an LDH cytotoxicity detection kit (Takara Bio Inc., Shiga, Japan) and Caspase-Glo® 3/7 Assay (Promega, Madison, WI, USA), according to the manufacturer's instructions. The cytotoxicity was evaluated by measuring the LDH activity and caspase-3 and -7 activities in the medium. Total LDH activity was defined as LDH activity in the medium containing 1% Triton X-100. LDH release (percentage) represents (LDH activity − LDH activity of control)/(total LDH activity − LDH activity of control) × 100.

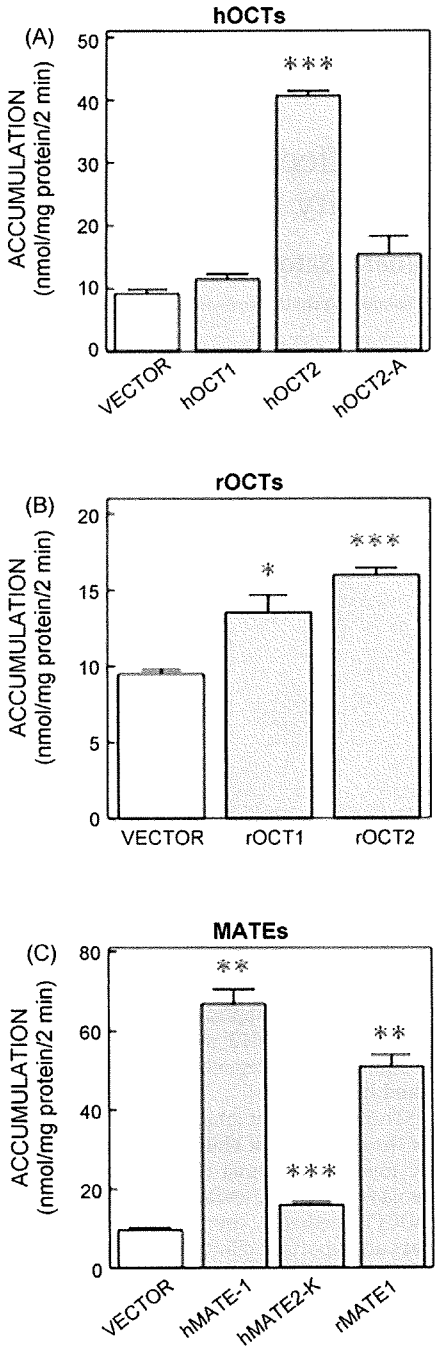

Fig. 1. Creatinine uptake by organic cation transporters. (A) HEK293 cells transfected with the empty vector, hOCT1, hOCT2, and hOCT2-A. (B) HEK293 cells transfected with the empty vector, rOCT1, and rOCT2. Cells transfected with hOCTs and rOCTs were incubated for 2 min at pH 7.4 at 37 °C with 10 μM [^{14}C]creatinine. (C) HEK293 cells transfected with the empty vector, hMATE1, hMATE2-K, and rMATE1. Cells transfected with MATEs were preincubated with incubation medium (pH 7.4) in the presence of 30 mM ammonium chloride for 20 min. The preincubation medium was removed, and the cells were incubated for 2 min at pH 7.4 at 37 °C with 10 μM [^{14}C]creatinine. Each column represents the mean ± S.E. of three monolayers from a typical experiment.

2.5. Animals

Male Wistar/ST rats (8 weeks) were purchased from SLC Animal Research Laboratories (Shizuoka, Japan). The rats were fed normal pellet food ad libitum, and given water freely. They were administered via gavage with 50 mg/kg imatinib three times and/or intraperitoneally with 5 mg/kg cisplatin (Randa®; Nippon Kayaku Co., Ltd., Tokyo, Japan) once after the second administration of imatinib. These drug solutions were prepared at concentrations of 30 and 0.5 mg/mL, respectively. Control rats were administered with the same volume of Ringer's solution. Three days after administration, the rats were maintained in metabolic cages for 24 h to determine the urinary levels of creatinine and urine output. Ninety-six hours after the administration of cisplatin, plasma, bladder urine, and kidneys were collected. The excised kidneys were gently washed, weighed, and homogenized in 9 volumes of saline. The amount of platinum was measured by ICP-MS. The animal experiments were performed in accordance with the "Guidelines for Animal Experiments of Kyoto University." All protocols were previously approved by the Animal Research Committee, Graduate School of Medicine, Kyoto University.

2.6. Renal functional and histological studies

For the measurement of blood urea nitrogen (BUN), creatinine, and N-acetyl-β-D-glucosaminidase (NAG), we used commercial kits (BUN and creatinine; Wako Pure Chemical Industries; NAG; Shionogi & Co., Ltd., Osaka, Japan). Kidneys were fixed in ethyl Carnoy's solution and stained with periodic acid-Schiff (PAS) reagent by Sapporo General Pathology Laboratory Co., Ltd. (Hokkaido, Japan).

2.7. Phamacokinetics of cisplatin

The pharmacokinetics experiment was performed using male Wistar/ST rats (8 weeks), as described previously with some modifications [4]. They were administered 50 mg/kg imatinib via gavage 3 h and just before cisplatin administration. Cisplatin (0.5 mg/kg) was administered as a bolus via the catheterized right femoral vein under pentobarbital anesthesia. Blood samples were collected at 0.5, 1, 1.5, 2, 2.5 and 3 min from the left femoral artery. Three minutes after the injection, the kidney was collected immediately after sacrificing the rats by blood loss. The excised tissues were gently washed, weighed and homogenized in 3 volumes of 0.9% NaCl. The amounts of cisplatin were measured by ICP-MS. At the same time, the concentration of imatinib was also determined using the high performance liquid chromatography (HPLC) method described below.

2.8. HPLC analysis for imatinib

The concentration of imatinib was determined using HPLC (model LC-10A; Shimadzu, Kyoto, Japan). HPLC analysis was performed as

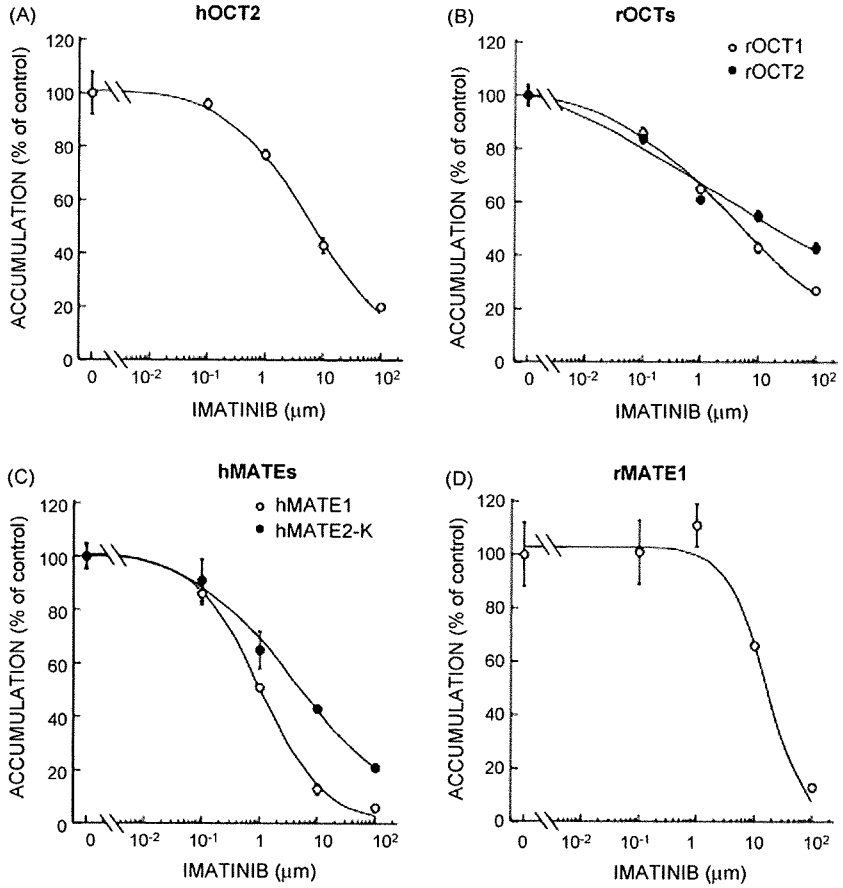

Fig. 2. Effect of imatinib on [^{14}C]creatinine uptake by HEK293 cells transiently expressing organic cation transport systems. (A) HEK293 cells transfected with hOCT2. (B) HEK293 cells transfected with rOCT1 (open circle) and rOCT2 (closed circle). (C) HEK293 cells transfected with hMATE1 (open circle) and hMATE2-K (closed circle). (D) HEK293 cells transfected with rMATE1. Cells were incubated with 20 μM [^{14}C]creatinine for 2 min at pH 7.4 at 37 °C in the presence of various concentrations of imatinib. For kinetic analyses, ammonium chloride (30 mM, pH 7.4, 20 min) was used to achieve intracellular acidification (C and D). Each point represents the mean ± S.E. of three monolayers from a typical experiment in several separate experiments.

described previously with some modification [14]. Separation was performed using a reversed-phase column (TSK gel ODS-80TM, 5-μm particle size, 150 mm × 4.6 mm i.d.; TOSOH, Tokyo, Japan) at 40 °C. Imatinib was detected by UV absorption at 267 nm.

2.9. Statistical analysis

Data are expressed as the mean ± S.E. Data were analyzed statistically using an unpaired t test or Bonferroni's multiple comparison test after one-way ANOVA. Significance was set at $P < 0.05$. In all figures except Fig. 6, where error bars are not shown, they are smaller than the symbols.

3. Results

3.1. Effect of imatinib on [^{14}C]creatinine uptake by HEK293 cells transiently expressing hOCT1, hOCT2, hOCT2-A, rOCT1, rOCT2, hMATE1, hMATE2-K and rMATE1

Based on our previous reports [4,5], the affinities of organic cation transporters against cisplatin were markedly low compared to tetraethyl ammonium, a typical substrate for organic cation transporters. Therefore, we chose low affinity substrate creatinine as a probe substrate for mimicking the interaction between cisplatin and imatinib via renal rOCT2 and hOCT2 [15].

First, we examined creatinine transport by organic cation transport systems. Consistent with previous reports, creatinine transport was stimulated by the expressions of hOCT2, rOCT1, rOCT2, hMATE1, hMATE2-K and rMATE1 (Fig. 1). Next, the inhibitory effect of imatinib on creatinine transport by these transporters was examined. The apparent IC_{50} values of imatinib on creatinine transport via hOCT2, rOCT1, rOCT2, hMATE1, hMATE2-K and rMATE1 were (in μM) 6.7, 4.1, 1.3, 1.0, 4.3, 16.6, respectively (Fig. 2). Therefore, we chose 10 μM imatinib as a potent inhibitor in the following experiments.

3.2. Effects of imatinib on cisplatin-induced cytotoxicity in HEK293 cells transiently expressing basolateral organic cation transporters, hOCT1, hOCT2, rOCT1, and rOCT2

To assess the cytotoxicity of cisplatin, LDH assay and caspase 3/7 assay were employed. Results from the LDH assay as well as the

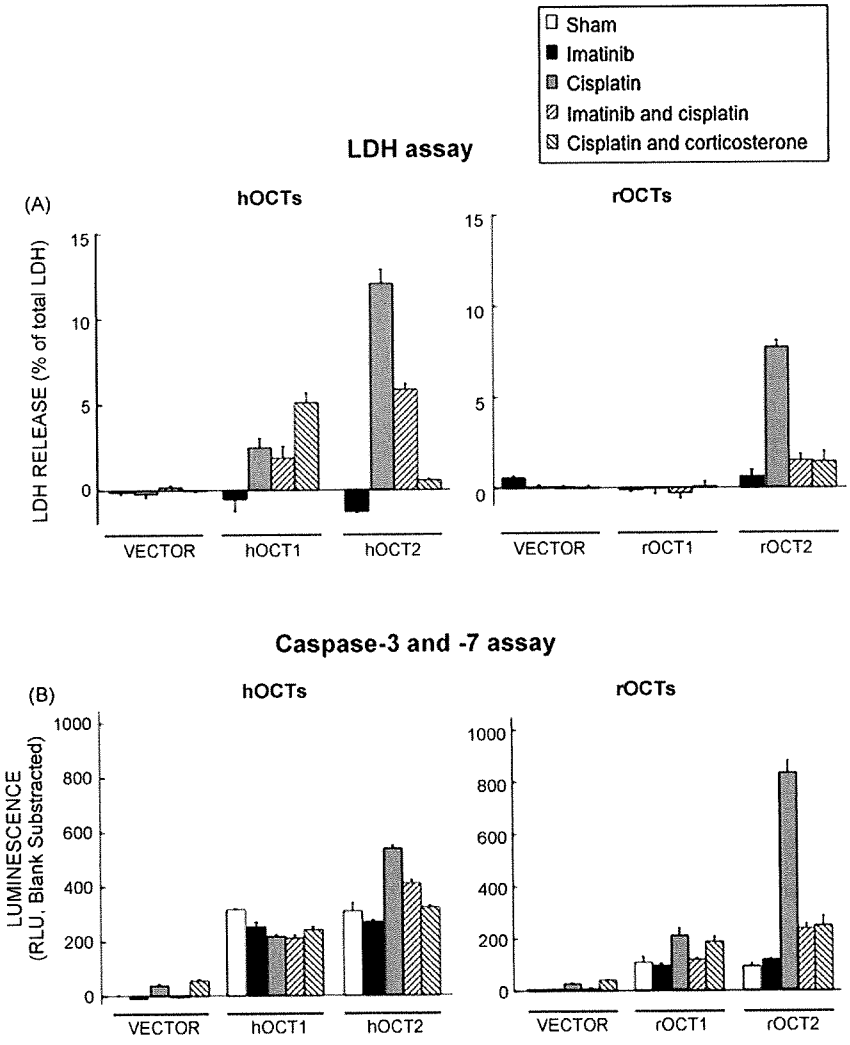

Fig. 3. Effect of imatinib on cisplatin-induced cytotoxicity in HEK293 cells transiently expressing basolateral organic cation transporters. HEK293 cells were transfected with empty vector, hOCT1, hOCT2, rOCT1, or rOCT2. Cells were treated with medium containing imatinib (10 μM; black column) or cisplatin (50 μM) with or without imatinib (positive sloped column and gray column, respectively) or corticosterone (100 μM; negative sloped column) for 2 h and then incubated in normal medium for 24 h. LDH (A) or caspase-3 and -7 (B) released into the medium was measured. Each column represents the mean ± S.E. of three monolayers from a typical experiment in several separate experiments.

caspase 3/7 assay showed that cisplatin-induced cytotoxicity via both human and rat OCT2 was markedly reduced by concurrent treatment with imatinib (Fig. 3) ($P < 0.001$ except hOCT2 for caspase 3/7 assay; $P < 0.01$). Corticosterone, a potent antagonist of OCT2, also attenuated cisplatin-induced cytotoxicity (Fig. 3). However, both human and rat OCT1-mediated cytotoxicities by cisplatin were much lower than OCT2-mediated cytotoxicities and were not prevented in the presence of imatinib and corticosterone.

3.3. Effects of imatinib on cisplatin-induced cytotoxicity in HEK293 cells transiently expressing apical organic cation transporters, hMATE1, hMATE2-K, and rMATE1

The expressions of hMATE1, hMATE2-K and rMATE1 did not affect cisplatin-induced cytotoxicity in LDH assay (Fig. 4A). However, a slight significant increase of caspase-3 and -7 activities was observed by cisplatin treatment in HEK293 cells expressing hMATE1 and rMATE1 compared to sham treatment ($P < 0.01$ and $P < 0.001$, respectively) (Fig. 4B). In addition, these increase caused by cisplatin treatment significantly decreased by the presence of imatinib ($P < 0.001$, Fig. 4B).

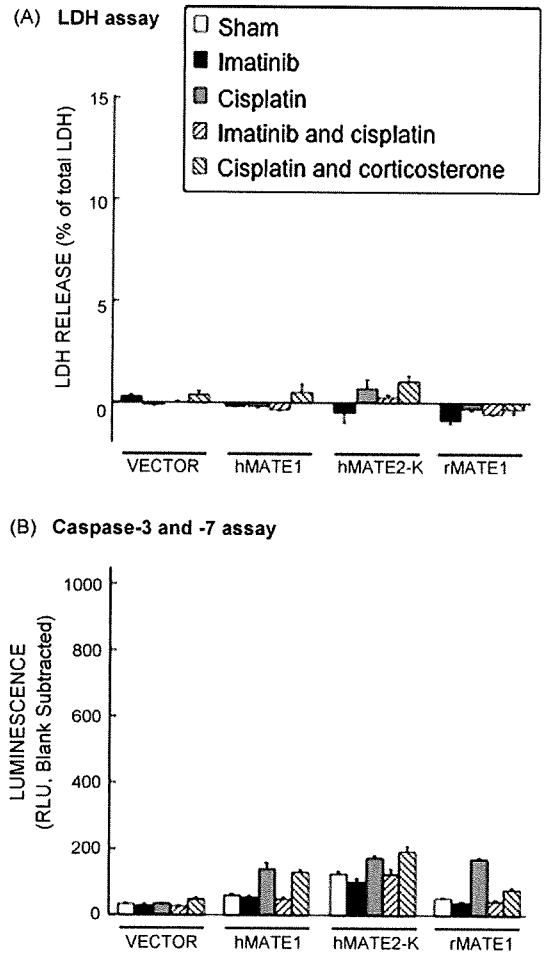

Fig. 4. Effect of imatinib on cisplatin-induced cytotoxicity in HEK293 cells transiently expressing apical organic cation transporters. HEK293 cells were transfected with empty vector, hMATE1, hMATE2-K, or rMATE1. Cells were treated with medium containing imatinib (10 μM; black column) or cisplatin (50 μM) with or without imatinib (positive sloped column and gray column, respectively) or corticosterone (100 μM; negative sloped column) for 2 h and then incubated in normal medium for 24 h. LDH (A) or caspase-3 and -7 (B) released into the medium was measured. Each column represents the mean ± S.E. of three monolayers from a typical experiment in several separate experiments.

3.4. Effects of imatinib on platinum accumulation in HEK293 cells transiently expressing basolateral organic cation transporters, hOCT1, hOCT2, rOCT1, and rOCT2

To obtain more information about the association between cisplatin-induced cytotoxicity and intracellular accumulation of

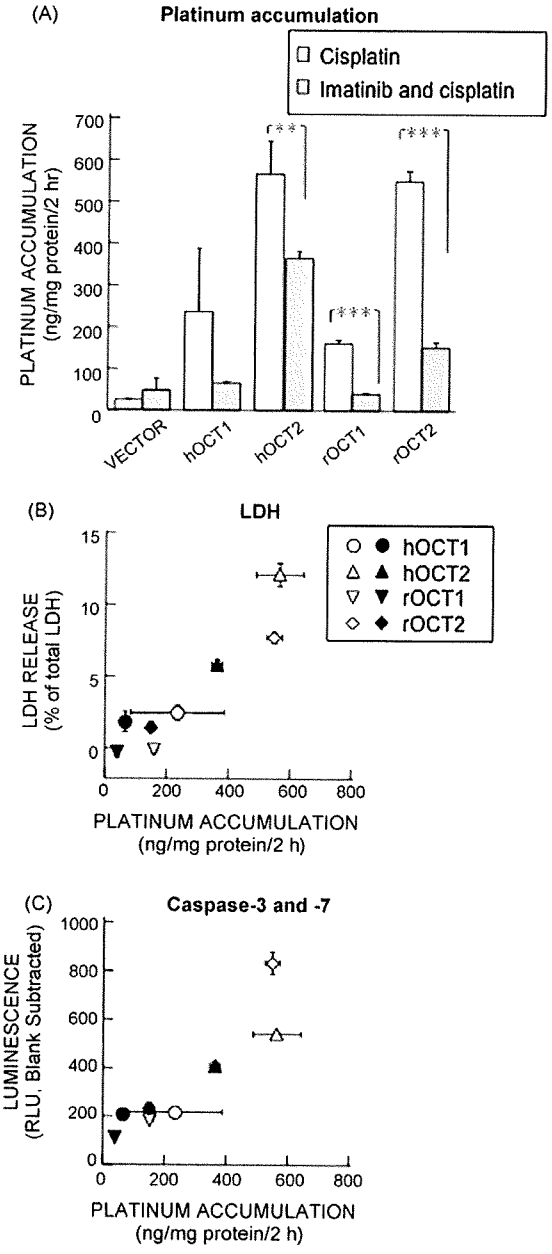

Fig. 5. Effect of imatinib on platinum accumulation in HEK293 cells transiently expressing basolateral organic cation transporters (A), and relation between platinum accumulation and cytotoxicity (B and C). (A) HEK293 cells were transfected with empty vector, hOCT1, hOCT2, rOCT1, or rOCT2. Cells were treated with medium containing cisplatin (50 μM) with or without imatinib (10 μM; closed column and open column, respectively) for 2 h. After washing, the cells were solubilized in 0.5 N NaOH, and the amount of platinum was determined by ICP-MS. Each column represents the mean ± S.E. of three monolayers. $^{**}P < 0.01$; $^{***}P < 0.001$, significantly different. (B and C) The data on LDH and caspase-3 and -7 are from Fig. 3. Platinum accumulation versus LDH release (B) or caspase-3 and -7 activities (C) on treatment with 50 μM cisplatin with or without imatinib (10 μM; closed symbol and open symbol, respectively).

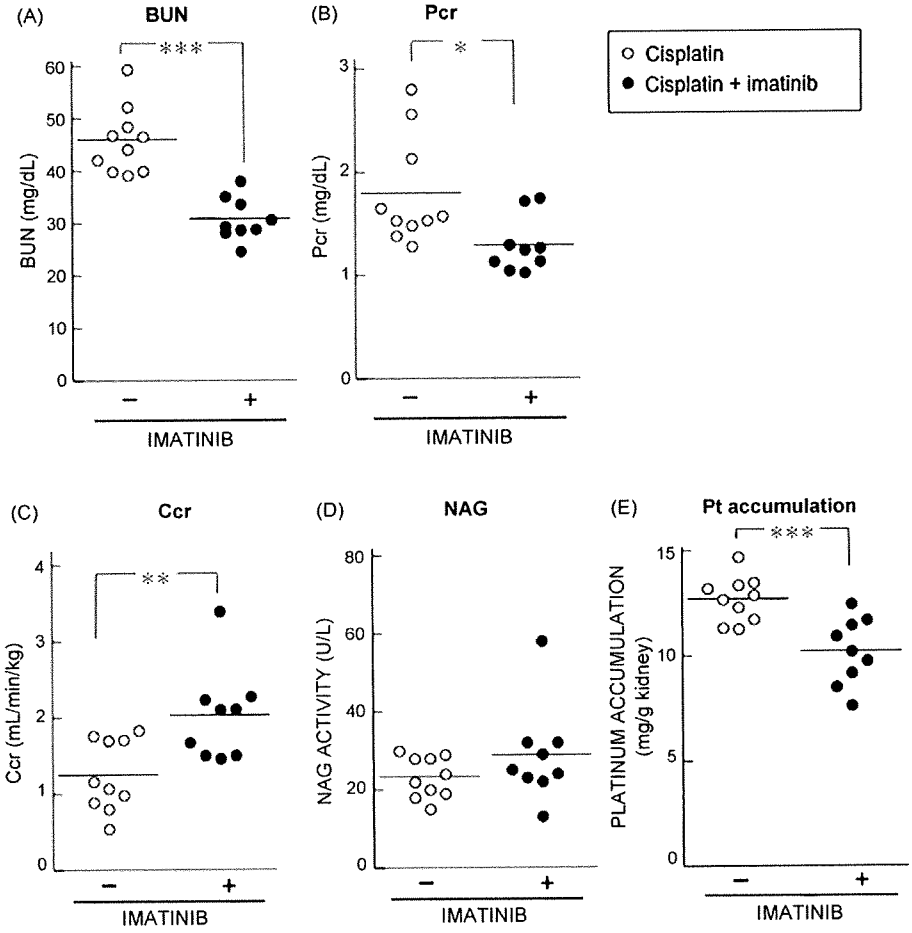

Fig. 6. Effect of coadministered imatinib on renal function and platinum accumulation of rats treated with cisplatin (5 mg/kg). Biochemical parameters (A: BUN; B: P_{cr}; C: C_{cr}; D: NAG) and platinum accumulation (E) in the kidney were examined on the fifth day after treatment with 5 mg/kg cisplatin with or without coadministration of 50 mg/kg imatinib. The kidney was homogenized in 9 volumes of buffer. Renal accumulation of platinum was then evaluated by ICP-MS. BUN, blood urea nitrogen; P_{cr}, plasma creatinine; C_{cr}, creatinine clearance; NAG, N-acetyl-β-D-glucosaminidase. Each bar represents the mean of nine or 10 rats from two independent experiments. $^{*}P < 0.05$; $^{**}P < 0.01$; $^{***}P < 0.001$, significantly different from cisplatin-treated rats.

cisplatin, we examined the effect of imatinib on platinum accumulation in HEK293 cells transiently expressing hOCT1, hOCT2, rOCT1 and rOCT2. Consistent with the results of cytotoxicity, platinum accumulation significantly decreased by the presence of imatinib in hOCT2- or rOCT2-expressing cells. In addition, imatinib decreased platinum accumulation in rOCT1-expressing cells, but accumulations via rOCT1 were less than a quarter of accumulations via rOCT2 (Fig. 5A). In combination of the data of cytotoxicity (Fig. 3) and cellular accumulation of cisplatin (Fig. 5A), the cellular cisplatin closely related with the magnitude of cytotoxicity with or without imatinib (Fig. 5B and C).

3.5. Effect of coadministrated imatinib on renal function and platinum accumulation of rats treated with cisplatin

Biochemical parameters on the 4 days after treatment in imatinib-treated rats were 13.0 ± 0.9 mg/dL (BUN), 0.42 ± 0.03 mg/dL (P_{cr}), 2.34 ± 0.20 mL/min (C_{cr}), and 26.4 ± 9.0 U/L (urinary NAG) (mean ± S.E. of five rats). These data were comparable with sham-operated rats (BUN, 13.1 ± 0.8 mg/dL; P_{cr}, 0.48 ± 0.08 mg/dL; C_{cr}, 1.77 ± 0.37 mL/min; urinary NAG, 23.7 ± 9.4 U/L, statistically not significant). Compared to the cisplatin-treated group, concurrent treatment with cisplatin and imatinib significantly reduced nephrotoxicity in BUN, P_{cr}, and C_{cr} (Fig. 6A–C). However, coadministered imatinib had no effect on the urinary NAG activity (Fig. 6D).

The renal accumulation of platinum was also measured 4 days after the intraperitoneal administration of 5 mg/kg cisplatin with or without gavage administration of 50 mg/kg imatinib. When rats were coadministered cisplatin with imatinib, the renal platinum accumulation decreased significantly compared to cisplatin alone (Fig. 6E).

3.6. Pharmacokinetics of cisplatin in rats coadministrated with imatinib

The pharmacokinetics of cisplatin in rats with or without the coadministration of imatinib was examined. Plasma concentrations of platinum up to 3 min after the bolus administration of cisplatin via the catheterized right femoral vein were determined (Fig. 7A). Imatinib (50 mg/kg) or Ringer's solution was administered via gavage 3 h before and in the final minute before the administration of cisplatin. The total clearance (CL_{total}) of cisplatin was significantly decreased in combined-modality rats (24.0 ± 1.1 mL/min) compared to cisplatin-treated rats (30.3 ± 1.3 mL/min) ($P < 0.01$) (Fig. 7B). The tissue uptake clearance (CL_{tissue}) of the kidney was also significantly decreased in combined-modality rats (1.7 ± 0.1 mL/min) compared to cisplatin-treated rats (2.2 ± 0.2 mL/min) ($P < 0.05$) (Fig. 7C). In

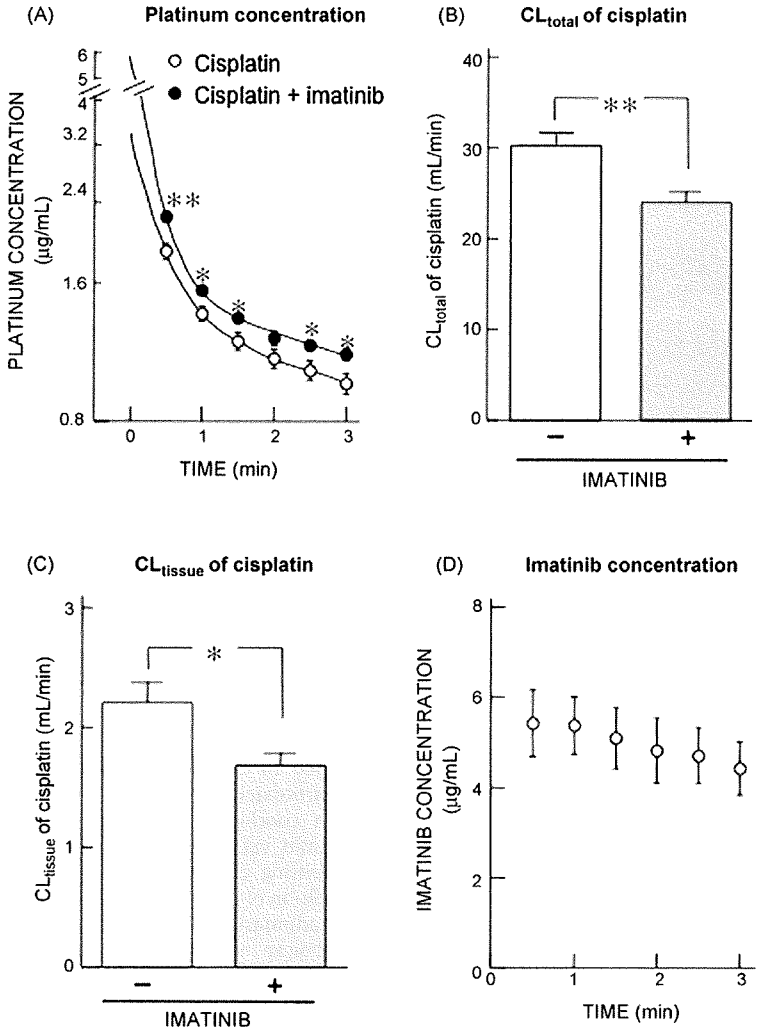

Fig. 7. Pharmacokinetics of cisplatin in rats coadministered with imatinib. (A) Plasma concentrations of platinum at various points were determined in male rats treated with cisplatin with or without coadministration of imatinib (closed circle and open circle, respectively). Total clearance (CL_{total}; B) and tissue uptake clearance (renal CL_{tissue}; C) were calculated by dividing the administered dose or the amount in tissue at 3 min by the area under the curve (AUC) from 0 to 3 min, respectively. (D) Plasma concentrations of imatinib at various points were determined in male rats treated with cisplatin with coadministration of imatinib (open circle). Each column represents the mean ± S.E. of 10 rats from two independent experiments. $^*P < 0.05$; $^{**}P < 0.01$, significantly different from cisplatin-treated rats.

addition, the plasma concentration of imatinib during 3 min was stable around 5 μg/mL (8 μM) (Fig. 7D), and the renal concentration of imatinib was 182 ± 22 μg/mL (309 ± 37 μM, mean ± S.E. of 10 rats).

3.7. Histology of rat kidney coadministered cisplatin with imatinib

The pathology of the rat kidney treated with cisplatin with or without coadministration of imatinib was examined (Fig. 8). The degeneration of tubular cells, including tubular dilatation, tubular cell vacuolation, tubular cell detachment from the basement membrane and brush-border detachment, was prominent in rats treated with cisplatin (Fig. 8A and B). These changes were seen to a lesser degree in the rat kidney after the coadministration of cisplatin and imatinib (Fig. 8C and D).

4. Discussion

For more than four decades, there has been no successful treatment to avoid cisplatin-induced nephrotoxicity while maintaining its strong anticancer efficacy. Only diuretics in combination with hydration of more than 4000 mL/day are used in the present clinical practice to prevent its severe nephrotoxicity. However, the continuous urge to urinate reduces patients' quality-of-life. Previously, the renal toxicity of cisplatin was suggested to be a result of rOCT2-mediated extensive renal accumulation from the circulation, and weak tubular secretion into the urine by rMATE1 in rats [16]. The preventative effect of imatinib against cisplatin-induced nephrotoxicity may be the first effective treatment to maintain its anticancer effect without hydration. In addition, combination therapy with imatinib may bring additional anticancer effects in some ABL or c-kit-positive tumors.

Peng et al. [17] reported that the mean peak plasma concentration of imatinib ranged from 72 ng/mL (0.12 μM; at a dose of 25 mg) to 3016 ng/mL (5.11 μM; at a dose of 750 mg) after once-daily administration and from 2315 ng/mL (3.93 μM; 800 mg/day) to 3880 ng/mL (5.73 μM; 1000 mg/day) after twice-daily administration. Considering the IC_{50} values of imatinib against renal organic cation transporters (<10 μM), the present concentration of imatinib is reasonable compared to its clinical use. In the pharmacokinetic study (Fig. 7D), the plasma concen-